

SUPPLEMENTAL INFORMATION (SI)

Suppression of Deletion Mutation in the Gene Encoding Essential PBP2b Reveals a New Lytic Transglycosylase Involved in Peripheral Peptidoglycan Synthesis in *Streptococcus pneumoniae* D39

Ho-Ching Tiffany Tsui^{#1}, Jiaqi J. Zheng^{#1}, Ariel N. Magallon¹, John D. Ryan¹, Rachel Yunck², Britta E. Rued¹, Thomas G. Bernhardt² and Malcolm E. Winkler^{1*}

¹Department of Biology, Indiana University Bloomington, Bloomington, IN 47405 and

²Department of Microbiology and Immunology, Harvard Medical School, Boston, MA 02115, USA

[‡]Contributed equally to this work

*Corresponding author

SUPPLEMENTAL EXPERIMENTAL PROCEDURES

SUPPLEMENTAL TABLE S1. Bacterial strains used in this study

SUPPLEMENTAL TABLE S2. Oligonucleotide primers used in this study

SUPPLEMENTAL TABLE S3. Structural similarity of extracellular domain of MltG_{Spn} to known protein structures

SUPPLEMENTAL TABLE S4. Genes encoding proteins with known or putative PG lytic domains and WalRK-regulated genes in *S. pneumoniae* serotype 2 strain D39, observed hydrolase activities in zymogram assays and phenotypes of deletion mutants in a $\Delta pbp1a \Delta mltG$ background.

SUPPLEMENTAL FIGURE LEGENDS: Fig. S1-S15

REFERENCES TO SUPPLEMENTAL INFORMATION

29 **SUPPLEMENTAL EXPERIMENTAL PROCEDURES**

30 ***Reconstruction of Δpbp2b strains with original mltG suppressor alleles (Fig. S4)***

31 Genotypes of strains in these constructions are listed in Table S1 and primers used
32 in constructions are compiled in Table S2. Two approaches were used to reconstruct
33 $\Delta pbp2b$ strains with *mltG* suppressor alleles (see Fig. S4). The first approach used
34 intermediate strains with insertions of a P_c -[*kan-rpsL*⁺] cassette either upstream or
35 downstream *mltG* in a *pbp1a*⁺ genetic background. This approach was only successful
36 in reconstructing $\Delta pbp2b sup3$ (IU9783, $\Delta pbp2b mltG(Y488D)$). To obtain IU9783, an
37 intermediate strain IU8986 (D39 $\Delta cps rpsL1 mltG^+-P_c$ -[*kan-rpsL*⁺]) with an insertion of
38 P_c -[*kan-rpsL*⁺] cassette immediately after *mltG* was constructed. An *mltG(Y488D)*
39 amplicon was obtained using IU7567 as a template and primers P1348 and P1349 and
40 transformed into IU8986 to obtain IU9760, which was sequenced to confirm the Y488D
41 change, and no other mutation in *mltG* or *pbp1a*. IU9760 was transformed with
42 $\Delta pbp2b<>aad9$ from IU7397 to obtain IU9783 (D39 $\Delta cps rpsL1 mltG(Y488D)$
43 $\Delta pbp2b<>aad9$) (Fig. S4).

44 We attempted a similar strategy to reconstruct the other suppressor strains without
45 success. The transformation of a *mltG*(Δ5bp) amplicon into IU8986 (*mltG*⁺- P_c -[*kan-*
46 *rpsL*⁺]) and the transformation of *mltG*(Δ488bp) or *mltG*(Ω45bp)² amplicons into IU8980
47 (P_c -[*kan-rpsL*⁺]-*mltG*⁺) yielded only strains with the wild-type *mltG* sequence. One
48 isolate was found to contain the *mltG*(Δ488bp) mutation, but it was found to also contain
49 a frameshift mutation in *pbp1a*.

50 The second approach (Fig. S4) was to transfer the *mltG* [Δ5bp, Δ488bp or (Ω45bp)²]
51 mutations into a stabilizing $\Delta pbp1a$ genetic background as the first step (see *Results*).

52 Amplicons were synthesized from the original suppressor strains as templates using
53 primers P1348 and P1349 and transformed into strain IU7325 ($\Delta cps\ rpsL1\ \Delta pbp1a$
54 $\Delta mltG::P_c-[kan-rpsL^+]$). The resulting stains were transformed with the $\Delta pbp2b<>aad9$
55 amplicon. The $\Delta pbp1a$ mutations in strains IU8565, IU8567 and IU8569 were repaired
56 by transformation first with a $\Delta pbp1a::P_c-[kan-rpsL^+]$ amplicon, followed by
57 transformation with a $pbp1a^+$ amplicon. Strains IU9777, IU9905 and IU9907 were
58 sequenced to confirm the correct *mltG* mutation and no initial mutation in *pbp1a*.

59

60 **Reconstruction of *pbp1a* alleles in a clean genetic background (Fig. 3)**

61 PCR amplicons containing *pbp1a* alleles from original $\Delta mltG$ suppressor strains
62 IU7258 ($\Delta mltG\ pbp1a$ (G494E)), IU7260 ($\Delta mltG\ pbp1a$ (G deletion at Gly451)), IU7286
63 ($\Delta mltG\ pbp1a$ (S89F)), IU7287 ($\Delta mltG\ pbp1a$ (A deletion at Lys160)), IU7288 ($\Delta mltG$
64 *pbp1a* (T insertion at Phe33)) were prepared from strain lysates and primers P234 and
65 P235. Amplicons were transformed into intermediate strain IU6726 (D39 $\Delta cps\ rpsL1$
66 $\Delta pbp1a::P_c-[kan-rpsL^+]$) as described above (see Fig. S4). The resulting strains were
67 designated IU7837 (*pbp1a* (G494E)), IU7839 (*pbp1a* (G deletion at Gly451)), IU7840
68 (*pbp1a* (S89F)), IU7843 (*pbp1a* (A deletion at Lys160)), and IU7845 (*pbp1a* (T insertion
69 at Phe33)). *pbp1a* alleles in reconstructed strains were confirmed by DNA sequencing.
70 A markerless $\Delta pbp1a$ allele in strain IU6741 was constructed by transforming a $\Delta pbp1a$
71 fusion amplicon containing 60 bp (20 codons) from the N-terminus and 60 bp (20
72 codons) from the C- terminus of *pbp1a* into strain IU6726 (see top, Fig. S4). The short
73 regions at the beginning and end of *pbp1a* were included in the $\Delta pbp1a$ allele to
74 maintain possible translational coupling of closely spaced pneumococcal genes.

75 ***Construction of zinc-dependent MltG merodiploid strain IU9102 (Fig. 3 and 6)***

76 The $\Delta bgaA::tet$ -P_{Zn}-RBS_{mltG}-*mltG* fusion amplicon was obtained by fusion PCR of a
77 5' PCR fragment containing *bgaA'::tet*-P_{Zn} (*bgaA'::tet*-P_{CZCD}) DNA template from pJWV25
78 (Eberhardt *et al.*, 2009)), a middle fragment containing RBS_{mltG}-*mltG* (24bp upstream
79 and ORF sequences of *mltG*), and 3' fragment of flanking *bgaA'* sequence. The fusion
80 amplicon was transformed into IU1945 to obtain strain IU8872 (D39 Δcps $\Delta bgaA::tet$ -
81 P_{Zn}-RBS_{mltG}-*mltG*). A $\Delta mltG::P_c$ -*aad9* fusion amplicon was transformed into IU8872 to
82 obtain zinc-dependent, merodiploid strain IU9102 (D39 Δcps $\Delta mltG::P_c$ -
83 *aad9*/ $\Delta bgaA::tet$ -P_{Zn}-RBS_{mltG}-*mltG*). IU9102 was maintained in media containing 0.2
84 mM ZnCl₂ and 0.02 mM MnSO₄ during all steps in the transformation procedure, single
85 colony isolation, and growth for storage. MnSO₄ was added at a concentration of 0.1X
86 of ZnCl₂ in all media to minimize Zn⁺² toxicity (Jacobsen *et al.*, 2011). Growth and cell
87 morphology of wild type strain IU1945 in BHI media containing 0.2 mM ZnCl₂ and 0.02
88 mM MnSO₄ is similar to growth in BHI media without additional ZnCl₂ and MnSO₄.

89

90 ***Construction of markerless ftsZ-L₂-mKate2, gfp-L₁-mltG, and double ftsZ-L₂-***
91 ***mKate2 gfp-L₁-mltG strains (Fig. 9)***

92 mKate2 is a far-red monomeric fluorescent protein, whose codons have been
93 optimized for expression in *S. pneumoniae* (Beilharz *et al.*, 2015). Because of its
94 relative stability, mKate2 is preferred over mCherry for localization studies. To construct
95 a markerless carboxyl fusion of *ftsZ* to *mKate2*, intermediate strain IU7614 (*ftsZ*⁺-P_c-
96 [*kan-rpsL*⁺]) was constructed by insertion of the P_c-[*kan-rpsL*⁺] cassette after the *ftsZ*
97 stop codon. The P_c-[*kan-rpsL*⁺] cassette was followed by a duplicated 60 bp of the 3'-

98 end of *ftsZ* and the downstream gene *yImE*. An *ftsZ-L₂-mKate2* fusion amplicon with
99 *ftsZ* replaced by *ftsZ-L₂-mKate2*, followed by 17 bp of the 3'-end of *ftsZ* was constructed
100 and transformed into strain IU7614 to obtain IU9148 (*ftsZ-L₂-mKate2*). The L₂ linker
101 sequence KLDIEFLQ was used for the C-terminal fusion as described in (Fleurie *et al.*,
102 2014).

103 To construct a markerless N-terminal fusion of *gfp* to *mItG*, intermediate strain
104 IU8980 (P_c[*kan-rpsL*⁺]-*mItG*⁺) was constructed with the P_c[*kan-rpsL*⁺] cassette placed
105 80 bp upstream of *mItG*. A *gfp-L₁-mItG* fusion amplicon with *mItG* replaced by *gfp-L₁-*
106 *mItG* was constructed and transformed into IU8980 to obtain IU10228 (*gfp-L₁-mItG*).
107 The original *mItG* start codon TTG is replaced with ATG of *gfp*. The L₁ linker sequence
108 LEGSG was used for the N-terminal fusion as described in (Fleurie *et al.*, 2014). The
109 DNA template for *gfp* is pUC57-*gfp(Sp)* (Martin *et al.*, 2010), which was codon
110 optimized for *S. pneumoniae* and has an aa substitution (A206K) that prevents GFP
111 dimerization.

112 To construct double *ftsZ-L₂-mKate2* *gfp-L₁-mItG* strain IU10353, IU10228 (*gfp-L₁-*
113 *mItG*) was transformed with the *ftsZ*⁺-P_c-[*kan-rpsL*⁺] amplicon from IU7614 to obtain
114 IU10318 (*gfp-L₁-mItG ftsZ*⁺-P_c-[*kan-rpsL*⁺]). IU10318 was tranformed with a *ftsZ-L₂-*
115 *mKate2* amplicon from IU9148 to obtain final strain IU10353.

116

117 ***Construction of mItG(ΔDUF_1346) strains***

118 Initially we did not known whether the DUF_1346 domain was essential for MltG
119 function. Since Δ*mItG* Δ*pbp1a* strains are viable, whereas Δ*mItG* *pbp1a*⁺ strains are not,
120 a *mItG(ΔDUF_1346)* mutation was first constructed in strain IU6741 (D39 Δ*cps rpsL* 1

121 $\Delta pbp1a$). IU6741 was transformed with $\Delta mltG::P_c\text{-}[kan-rpsL^+]$ from strain K637,
122 producing strain IU7325 (D39 $\Delta cps\ rpsL1\ \Delta pbp1a\ \Delta mltG::P_c\text{-}[kan-rpsL^+]$). A
123 $mltG(\Delta DUF_1346)$ fusion amplicon was then constructed by fusion PCR and
124 transformed into IU7325. The resulting strain was designated as IU8910 (D39 Δcps
125 $rpsL1\ \Delta pbp1a\ mltG(\Delta DUF_1346)$). To evaluate whether the $mltG(\Delta DUF_1346)$ allele is
126 functional in IU8910, we attempted to transform a $\Delta pbp2b$ amplicon (Table 2) into
127 IU8910. No colonies were recovered, indicating that $MltG(\Delta DUF_1346)$ is functional in
128 IU8910.

129 We synthesized an $mltG(\Delta DUF_1346)$ amplicon from strain IU8910 and transformed
130 the amplicon into strain IU8980 ($P_c[kan-rpsL^+]\text{-}mltG^+$). Hundreds of well-formed
131 streptomycin resistant colonies appeared after 20 hours of incubation. Two isolates
132 (strain IU9025 and IU9026) were stored from independent transformations, and DNA
133 sequencing confirmed that both strains contain the $mltG(\Delta DUF_1346)$ allele. DNA
134 sequencing also confirmed that $pbp1a^+$ of strain IU9025 had not accumulated any
135 mutations.

136

137 ***Conditions comparing growth of $mltG^+$ and $mltG(\Delta DUF_1346)$ strains (Fig. S9)***

138 Growth of $mltG^+$ parent strain IU1824 and $mltG(\Delta DUF_1346)$ mutant IU9025 was
139 compared in media containing high salt, β -lactam antibiotic penicillin G, and at low pH.
140 To test growth in high salt conditions, IU1824 and IU9025 were grown in BHI broth
141 without additional NaCl (0.08 M NaCl in BHI formula), or in BHI broth with additional
142 NaCl to a final concentration of 0.3 M. Strains were grown overnight in BHI broth, and
143 diluted to $OD_{620} \approx 0.003$ in BHI broth with or without additional NaCl. To test the growth

of IU1824 and IU9025 in the presence penicillin G, strains were grown overnight in BHI broth, and diluted to $OD_{620} \approx 0.003$ in BHI broth for culture growth. At $OD_{620} \approx 0.1$, penicillin G sodium salt (Sigma PEN-NA) was added to the cultures to final concentrations of 0, 0.004 (0.5x MIC, Kocaoglu *et al.*, 2015), and 0.006 $\mu\text{g}/\text{ml}$. This experiment was repeated once with addition of penicillin G concentrations of 0, 0.002, 0.004 and 0.008 $\mu\text{g}/\text{ml}$. To test the growth of IU1824 and IU9025 at low pH condition, strains were grown overnight in BHI broth (pH 7.2), and diluted to $OD_{620} \approx 0.003$ in BHI broth for culture growth. At $OD_{620} \approx 0.1$, 100 or 150 μL of 1 M HCl were added to the 5 mL cultures to decrease the pH to 5.8 or 5.0. This growth experiment was repeated once. To test the effect of temperature on growth of *mltG⁺* and *mltG(ΔDUF_1346)* strains, ice from frozen cultures of both strains was streaked onto two TSAII-BA plates. One plate was incubated at 37°C in an atmosphere of 5% CO₂ overnight, and the other was incubated at 42°C in an atmosphere of 5% CO₂ overnight. The size and morphologies of the colonies of the two strains were compared.

159 ***Western blotting (Fig. S2)***

Strains were grown exponentially in BHI broth to $OD_{620} \approx 0.15$. Lysates were prepared as described previously (Wayne *et al.*, 2012) and separated using 10 % or 4-15% mini-protean TGX pre-cast gels (Bio-Rad). FLAG-, HA-, and Myc-tagged proteins were detected by Western blotting as described previously (Tsui *et al.*, 2014). Chemiluminescent signal in protein bands was quantitated by using an IVIS imaging system as described in (Wayne *et al.*, 2010).

167 **DNA library construction, Illumina MiSeq DNA sequencing, and bioinformatic**
168 **analyses (Table 1)**

169 One µg of genomic DNA of each sample was diluted to 130 µL with TE and sheared
170 using the following settings on the S220 focused-ultrasonicator (Covaris): 105W Peak
171 Incident Power; 5 % Duty Factor, 200 Cycles Per Burst; 40 seconds Treatment Time.
172 Sheared samples were purified using AmpureXP beads (Agencourt/Seradyn/Beckman
173 Coulter, A63881) to sample ratio of 0.5X and eluted with 54 µL of EB (Qiagen). Sheared
174 samples were visualized using a D1K High Sensitivity tape (Agilent, 5067-5363) on an
175 Agilent 2200 TapeStation and consisted mostly of ≈650 to 700 bp fragments. Library
176 construction was carried out on the Biomek FX^P (Beckman Coulter) using a modified
177 SWHT (SPRIworks High Throughput for Illumina, Beckman Coulter) method to
178 accommodate a 700 bp distribution. Bioo Scientific NextFlex DNaseq Library Kit for
179 Biomek FX^P (5140-42) was used in conjunction with Bioo Scientific NextFlex DNA
180 barcodes-96 adaptors (514105). Following library construction, 15 µL of the 25 µL pre-
181 enrichment library was used as template in a 10-cycle PCR amplification. Library sizes
182 and concentrations were determined using TapeStation and Quant-iT Picogreen
183 (Molecular Probes, P7589), respectively. Dilutions were made to 20 nM and pooled in
184 preparation for a MiSeq run. 30 µL of 20 nM library was diluted to 500 µL using Illumina
185 buffer HT1 and loaded onto a 500 cycle MiSeq (version 2) flowcell (Illumina, MS-102-
186 2003). Paired-end run cycle parameters were 260 (Read1) + 8 (Index read) + 260
187 (Read2). DNA sequences were assembled based on the published encapsulated D39
188 genome sequence (Lanie *et al.*, 2007). Bioinformatic analyses was performed using
189 cutadapt (<https://code.google.com/p/cutadapt/>) with a min length of 100 and quality

190 cutoff of 30, and assembled using newbler (Margulies *et al.*, 2005), mapped using
191 bowtie (Langmead *et al.*, 2009) and called SNPs using mpileup (Li *et al.*, 2009). Full
192 coverage was obtained for the genomes of each mutant with >175 reads of most base
193 pairs. Gaps were only present at the expected *cps2A* to *cps2H* and *pbp2b* regions.

194

195 ***MltG* sequence alignment and secondary structure information (Fig. 5 and S6)**

196 The *MltG_{Eco}* sequence (gi accession 687676267) was aligned with the *MltG_{Spn}* (gi:
197 116076234) and *YceG_{Lmo}* (gi: 16803539) using Clustal Omega (Sievers *et al.*, 2011)
198 with default parameters. Secondary structure information of *MltG_{Eco}* was obtained from
199 the PDB database (PDB ID: 2R1F).

200

201 ***RNA-Seq analysis (Table 4)***

202 cDNA libraries were prepared from total RNA by the Center for Genomics and
203 Bioinformatics at Indiana University in Bloomington, Indiana. The mRNA was enriched
204 from 1 µg of total RNA using RiboZero™ rRNA Removal Kit (Bacteria) (EpiCentre, Inc.).
205 rRNA-depleted mRNA samples were purified using RNeasy Minelute Cleanup Kit
206 (Qiagen). Double-stranded cDNA synthesis was performed following ScriptSeq™
207 Complete Kit (Bacteria) Preparation guide (EpiCentre, Inc.) in accordance with the
208 manufacturer's standard protocol. Entire resultant mRNA sample was fragmented using
209 divalent cations via incubation for 5 min at 85°C. The first strand of cDNA was
210 synthesized by reverse transcription using random-sequence primers containing a
211 tagging sequence at their 5' ends. Di-tagged cDNA was synthesized by random
212 annealing of a terminal-Tagging Oligo to the 3' end of the cDNA for extension of the

213 cDNA by DNA polymerase. Di-tagged cDNA was purified using Agencourt AMPure® XP
214 beads (Beckman Coulter) followed by PCR amplification for 15 cycles using Failsafe™
215 PCR enzyme and ScriptSeq™ Index PCR Primer set (EpiCentre, Inc.). This step
216 generated the second strand of cDNA and completed the addition of Illumina adapter
217 sequences incorporating a user-defined barcode. The amplified libraries were purified
218 using Agencourt AMPure® XP beads. Quality and quantity were assessed using D1000
219 TapeStation (Agilent Technologies) and Quant-iT™ PicoGreen® dsDNA Assay Kit (Life
220 Technologies), respectively. Sequencing was performed at the Greehey Children's
221 Cancer Research Institute Genome Sequencing Facility at the University of Texas
222 Health Science Center at San Antonio, Texas. Cluster generation was performed using
223 TruSeq PE Cluster Kit v3-cBot-HS (Illumina). Single-end, 50 bp sequencing was
224 performed using TruSeq SBS Kit v3-HS (Illumina) on a HiSeq 2000 sequencer
225 (Illumina). Image analysis, base calling, sequencing reads de-multiplexing were
226 followed by default Illumina procedure.

227 The raw sequencing reads were quality and adapter trimmed using Trimmomatic
228 version 33 (Lohse *et al.*, 2012) with a minimum final read length of 35. The trimmed
229 reads were mapped onto the *S. pneumoniae* D39 (RefSeq NC_008533) genome and
230 D39 plasmid pDP1 sequence (RefSeq NC_005022) using bowtie2 version 2.1
231 (Langmead & Salzberg, 2012). Custom PERL scripts were used to generate read
232 counts for the genes and 100 bp non-overlapping intergenic regions of the genome.
233 Differential gene expression was identified using DESeq2 (version 1.8.1) (Love *et al.*,
234 2014) using default parameters (Robinson *et al.*, 2010). The false-discovery rate (FDR)
235 was calculated using Benjamini and Hochberg's algorithm (Benjamini & Hochberg,

236 1995) and a gene or region was defined as differentially expressed if it had an up- or
237 down-fold change of 1.8 and their FDR was less than 0.05.

238

239 **QRT-PCR analysis (Fig. S15)**

240 RNA from each strain was prepared as described in *Experimental procedures* for
241 RNA-Seq analysis. Five µg of purified RNA were further treated with DNA-free DNA
242 Removal Kit (Ambion). 125 ng of treated RNA were used to synthesize cDNA by qScript
243 Felex cDNA synthesis kit (Quanta Biosciences). RT-PCR was performed using the
244 Brilliant III Ultra-Fast SYBR Green qPCR Master Mix (Agilent Technologies). Each
245 reaction contained 10 µl of 2xBrilliant III Ultra-Fast SYBR Green QPCR Master Mix
246 (Agilent), 2 µl of each 2 µM primers (Table S2), 0.3 µl of a 1:500 dilution of ROX
247 reference dye and 6 µl of diluted cDNA. Samples were run in an MX3000P thermocycler
248 (Stratagene) with Program MxPro v. 3.0. QRT-PCR reactions were performed 3 times
249 each for three independent biological samples. The transcript amounts were normalized
250 to *gyrA* RNA amount (Table S2). Data were analyzed with the SYBR Green (with
251 dissociation curve) program on the thermocycler. Four dilutions of cDNA from a wild-
252 type *S. pneumoniae* strain were used to generate standard curves for each primer set.
253 For statistical analysis, normalized transcript amounts of *spd_1874*, *spd_0104*, and
254 *pcsB* were tested with a one sample t test (GraphPad Prism) to determine if the mean
255 was significantly different from a hypothetical value of 1.

256

257

258

259 ***Membrane preparation from S. pneumoniae cells for zymogram analysis (Fig. S8)***

260 Membrane preparations from strains IU1945 (D39 Δ cps parent), K5 (Δ lytC), K27
261 (Δ lytB) and K43 (Δ lytA) were made as previously described with minor modifications
262 (Wayne *et al.*, 2010). Briefly, 20 mL cultures of each strain were grown in BHI broth to
263 OD₆₂₀ ≈0.3. Cells were collected by centrifuging at 16,500 xg for 5 min at 4°C. Pellets
264 were washed with 2 mL 1 x SMM buffer (0.5 M sucrose, 20 mM MgCl₂, 20 mM MES pH
265 6.5) at room temperature and resuspended in 2 mL 1 x SMM buffer. 100 μ L of 10
266 mg/mL lysozyme (Sigma), 8 μ L of 1mg/mL of mutanolysin (Sigma), and 20 μ L of
267 protease inhibitor cocktail set III (Calbiochem) were added to each resuspended pellet,
268 and mixtures were incubated at 37°C for 1 hour to digest cell wall. Protoplasts were
269 collected as pellets following centrifugation at 8,000 xg for 10 min at room temperature.
270 Protoplast pellets were frozen on dry ice for 10 min and resuspended in 2 mL of cold
271 Buffer H (20 mM HEPES, pH 8.0, 200 mM NaCl, 1 mM DTT, and protease inhibitor
272 cocktail set III). 20 μ L of 0.1 M MgCl₂, 20 μ L of 0.1 M CaCl₂, 4 μ L of 5 mg/mL DNase
273 (Sigma), and 4 μ L of 10 mg/mL RNase (Sigma) were added to each resuspended pellet,
274 and the mixtures were incubated on ice for 1 h. Following centrifugation at 16,000 xg for
275 30 min at 4°C, the pellets were collected as membrane fractions, and were resuspended
276 in 60 μ L solubilization buffer (1% (wt/vol) SDS, 0.1% vol/vol Triton-X-100). 5 μ L was
277 taken for protein concentration determination with the DCTM protein assay kit (Bio-Rad).
278 Equal volumes of 2X Laemmli sample buffer (Bio-Rad, 161-0737) without added β -
279 mercaptoethanol, were added to the remaining membrane solutions. Mixtures were
280 incubated at 100°C for 10 min before loading into gel lanes for zymogram analysis.

282 **Zymogram analysis (Fig. S8)**

283 Zymogram analysis was performed with a protocol modified from Bartual *et al.*,
284 (2014). Lysed cell preparation from strain IU1945 was used as the PG substrate. 300
285 mL of strain IU1945 was grown up to $OD_{620} \approx 0.3$ in BHI broth and collected by
286 centrifugation at 10,000 xg for 10 min at 4 °C. Pellets were washed once with 5 mL of
287 ice-cold buffer containing 100 mM NaCl, 20 mM Tris-HCl pH 7.4 buffer, and
288 resuspended in 1.5 mL of the same buffer. Resuspended cells were incubated at 100 °C
289 for 10 min, followed by centrifugation at 16,000 xg for 10 min. The pellet was
290 resuspended in 1.5 mL of 1.5 M Tris-HCl, pH 8.8 and stored at -20 °C. The 1.5 mL
291 suspension of lysed IU1945 cells was added to a 12% SDS-PAGE resolving gel solution
292 (total volume 7.5 mL) containing 0.33 mL of 1.5 M Tris-HCl (pH 8.8), 75 µL of 10% SDS,
293 2.25 mL of 40% acrylamide (19:1 acrylamide/bis-acrylamide, A9926 Sigma), 3.3 mL
294 water, 37.5 µL 10% ammonium persulfate (APS) and 3.75 µL TEMED (Bio-Rad,
295 1610800). 4% SDS-PAGE stacking gel solution was made with a mixture of 470 µL of
296 0.5M Tris-HCl, pH 6.8, 19 µL of 10 %SDS, 190 µL of 40 % acrylamide, 1.2 mL water, 11
297 µL 10 % APS, and 1.1 µL TEMED. 35 µg of membrane proteins from strains IU1945,
298 K7, K27 or K43, or 10 µL of PageRuler prestained protein ladder (Thermo Scientific)
299 was loaded into each lane. Gel electrophoresis was performed in Tris-glycine SDS
300 buffer for 3h at 150V. The gel was washed with distilled water twice for 30 min each and
301 incubated in \approx 300 mL of refolding buffer (50 mM NaCl, 20 mM MgCl₂, 0.5% (vol/vol)
302 Triton X-100, and 20 mM Tris-HCl, pH 7.4) with gentle shaking at 37 °C for 12 to 14 h.
303 Gel images were obtained by photography against a black background.

TABLE S1. Bacterial strains used in this study^a

<i>S. pneumoniae</i> strains			
Strain number	Genotype (description) ^b	Antibiotic resistance ^c	Reference or source
IU1690	D39 <i>cps</i> ⁺	None	Lanie <i>et al.</i> , 2007
IU1751	R6 $\Delta mreCD \leftrightarrow aad9$	Spc ^R	Land and Winkler, 2011
IU1824	D39 <i>rpsL1</i> $\Delta cps2A'-cps2H' = D39\ rpsL1$ Δcps	Str ^R	Lanie <i>et al.</i> , 2007
IU1945	D39 $\Delta cps2A'-cps2H' = D39\ \Delta cps$	None	Lanie <i>et al.</i> , 2007
IU2519	D39 $\Delta bgaA'::kanT1t2-P_{fcsK}-pcsB^+$	Kan ^R	Barendt <i>et al.</i> , 2009
IU3286	D39 <i>rpsL1</i> $\Delta cps2E::P_c-[kan-rpsL^+]$	Kan ^R Str ^S	Ramos-Montanez <i>et al.</i> , 2010
IU3877	D39 $\Delta cps\ \Delta lytB \leftrightarrow P_c-[kan-rpsL^+]$	Kan ^R	Barendt <i>et al.</i> , 2011
IU3878	D39 $\Delta cps\ \Delta spd_0873 \leftrightarrow P_c-[kan-rpsL^+]$	Kan ^R	Barendt <i>et al.</i> , 2011
IU3897	D39 $\Delta cps\ \Delta mreCD \leftrightarrow P_c erm$	Erm ^R	Land & Winkler, 2011
IU4970	D39 $\Delta cps\ mreC-L-FLAG^3-P_c erm$	Erm ^R	Land & Winkler, 2011
IU6647	D39 $\Delta cps\ \Delta pbp1a::P_c erm$ (IU1945 X $\Delta pbp1a::P_c erm$ from E177)	Erm ^R	This study
IU6649	D39 $\Delta cps\ \Delta pbp1b::P_c erm$ (IU1945 X $\Delta pbp1b::P_c erm$ from E193)	Erm ^R	This study
IU6662	D39 $\Delta cps\ \Delta pbp1a::P_c-[kan-rpsL^+]$ (IU1945 X $\Delta pbp1a::P_c-[kan-rpsL^+]$ from K164)	Kan ^R	This study
IU6680	D39 $\Delta cps\ \Delta pbp2a::P_c-[kan-rpsL^+]$ (IU1945 X $\Delta pbp2a::P_c-[kan-rpsL^+]$ from K166)	Kan ^R	This study
IU6726	D39 $\Delta cps\ rpsL1\ \Delta pbp1a::P_c-[kan-rpsL^+]$ (IU1824 X $\Delta pbp1a::P_c-[kan-rpsL^+]$ from K164)	Kan ^R Str ^S	This study
IU6741	D39 $\Delta cps\ rpsL1\ \Delta pbp1a$ (IU6726 X fusion $\Delta pbp1a$)	Str ^R Kan ^S	This study
IU7258	D39 $\Delta cps\ \Delta mltG::P_c-[kan-rpsL^+]\ sup1$ (<i>pbp1a</i> (G494E)(GGA→GAA) (single colony isolate of K637))	Kan ^R	This study
IU7260	D39 $\Delta cps\ \Delta mltG::P_c erm\ sup1$ (<i>pbp1a</i> (ΔG at G451)(GGT ₁₇ G-T)(single	Erm ^R	This study

	colony isolate of E681)		
IU7286	D39 Δ cps Δ mltG::P _c -[kan-rpsL ⁺] sup2 (pbp1a (S89F)(TCT→TTT) (IU1945 X Δ mltG::P _c -[kan-rpsL ⁺] from IU7258)	Kan ^R	This study
IU7287	D39 Δ cps Δ mltG::P _c -[kan-rpsL ⁺] sup3 (pbp1a(ΔA at K160)(AAA→AA-)) (IU1945 X Δ mltG::P _c -[kan-rpsL ⁺] from IU7258)	Kan ^R	This study
IU7288	D39 Δ cps Δ mltG::P _c -erm sup2 (pbp1a(ΩT at F33)(TTC→TTTC))(IU1945 X Δ mltG::P _c -erm from IU7260)	Erm ^R	This study
IU7325	D39 Δ cps rpsL1 Δ pbp1a Δ mltG::P _c - [kan-rpsL ⁺] (IU6741 X Δ mltG::P _c -[kan- rpsL ⁺] from K637)	Kan ^R Str ^S	This study
IU7327	D39 Δ cps rpsL1 Δ pbp1a Δ mltG::P _c -erm (IU6741 X Δ mltG::P _c -erm from IU7260)	Erm ^R Str ^R	This study
IU7337	D39 Δ cps ΔbgaA::kan-t1t2-P _{fcsK} -pbp2b	Kan ^R	Tsui <i>et al.</i> , 2014
IU7397	D39 Δ cps Δpbp2b<>aad9//ΔbgaA::kan- t1t2-P _{fcsK} -pbp2b	Kan ^R Spc ^R	Tsui <i>et al.</i> , 2014
IU7399	D39 Δ cps mltG-HA-P _c -kan (IU1945 X fusion mltG-HA-P _c -kan)	Kan ^R	This study
IU7403	D39 Δ cps mltG-FLAG-P _c -erm (IU1945 X fusion mltG-FLAG-P _c -erm)	Erm ^R	This study
IU7405	D39 Δ cps mltG-Myc-P _c -kan (IU1945 X fusion mltG-Myc-P _c -kan)	Kan ^R	This study
IU7476	D39 Δ cps Δpbp2b<>aad9 sup1 (IU1945 X Δpbp2b<>aad9 from IU7397)	Spc ^R	This study
IU7477	D39 Δ cps Δpbp2b<>aad9 sup2 (IU1945 X Δpbp2b<>aad9 from IU7397)	Spc ^R	This study
IU7567	D39 Δ cps Δpbp2b<>aad9 sup3 (IU1945 X Δpbp2b<>aad9 from IU7397)	Spc ^R	This study
IU7570	D39 Δ cps Δpbp2b<>aad9 sup4 (IU1945 X Δpbp2b<>aad9 from IU7397)	Spc ^R	This study
IU7580	D39 Δ cps mreC-L-FLAG ³ -P _c -erm mltG- HA-P _c -kan (IU4970 X mltG-HA-P _c -kan from IU7399)	Kan ^R Erm ^R	This study
IU7582	D39 Δ cps mreC-L-FLAG ³ -P _c -erm mltG- Myc-P _c -kan (IU4970 X mltG-Myc-P _c - kan from IU7405)	Kan ^R Erm ^R	This study
IU7614	D39 Δ cps rpsL1 ftsZ ⁺ -P _c -[kan-rpsL ⁺] (IU1824 X fusion ftsZ ⁺ -P _c -[kan-rpsL ⁺])	Kan ^R Str ^S	This study
IU7765	D39 Δ cps Δpbp2b<>aad9 sup5 (IU1945 X Δpbp2b<>aad9 from IU7397)	Spc ^R	This study

IU7837	D39 $\Delta cps\ rpsL1\ pbp1a$ (G494E) (IU6726 X $pbp1a$ allele from IU7258)	Str ^R Kan ^S	This study
IU7839	D39 $\Delta cps\ rpsL1\ pbp1a$ (ΔG at G451) (IU6726 X $pbp1a$ allele from IU7260)	Str ^R Kan ^S	This study
IU7840	D39 $\Delta cps\ rpsL1\ pbp1a$ (S89F) (IU6726 X $pbp1a$ allele from IU7286)	Str ^R Kan ^S	This study
IU7843	D39 $\Delta cps\ rpsL1\ pbp1a$ (ΔA at K160) (IU6726 X $pbp1a$ allele from IU7287)	Str ^R Kan ^S	This study
IU7845	D39 $\Delta cps\ rpsL1\ pbp1a$ (ΩT at F33) (IU6726 X $pbp1a$ allele from IU7288)	Str ^R Kan ^S	This study
IU7850	D39 $\Delta cps\ \Delta pbp1b::P_c-[kan-rpsL^+]$ IU1824 X $\Delta pbp1b::P_c-[kan-rpsL^+]$ from K180	Kan ^R Str ^S	This study
IU7852	D39 $\Delta cps\ \Delta pbp2a::P_c-[kan-rpsL^+]$ IU1824 X $\Delta pbp2a::P_c-[kan-rpsL^+]$ from K166	Kan ^R Str ^S	This study
IU7931	D39 $\Delta cps\ rpsL1\ \Delta pbp1a\ mltG::P_c\text{-}erm$ $\Delta pbp2b<>aad9$ (IU7327 X $\Delta pbp2b<>aad9$ from IU7397)	Erm ^R Str ^R	This study
IU8549	D39 $\Delta cps\ rpsL1\ \Delta pbp1a\ mltG(\Delta 5bp)$ (IU7325 X $mltG(\Delta 5bp)$ from IU7477)	Str ^R Kan ^S	This study
IU8551	D39 $\Delta cps\ rpsL1\ \Delta pbp1a\ mltG(Y488D)$ (IU7325 X $mltG(Y488D)$ from IU7567)	Str ^R Kan ^S	This study
IU8553	D39 $\Delta cps\ rpsL1\ \Delta pbp1a\ mltG(\Delta 488bp)$ (IU7325 X $mltG(\Delta 488bp)$ from IU7570)	Str ^R Kan ^S	This study
IU8555	D39 $\Delta cps\ rpsL1\ \Delta pbp1a\ mltG(\Omega 45bp)^2$ (IU7325 X $mltG(\Omega 45bp)^2$ from IU7765)	Str ^R Kan ^S	This study
IU8565	D39 $\Delta cps\ rpsL1\ \Delta pbp1a\ mltG(\Delta 5bp)$ $\Delta pbp2b<>aad9$ (IU8549 X $\Delta pbp2b<>aad9$ from IU7397)	Str ^R Kan ^S Spc ^R	This study
IU8567	D39 $\Delta cps\ rpsL1\ \Delta pbp1a\ mltG(\Delta 488bp)$ $\Delta pbp2b<>aad9$ (IU8553 X $\Delta pbp2b<>aad9$ from IU7397)	Str ^R Kan ^S Spc ^R	This study
IU8569	D39 $\Delta cps\ rpsL1\ \Delta pbp1a\ mltG(\Omega 45bp)^2$ $\Delta pbp2b<>aad9$ (IU8555 X $\Delta pbp2b<>aad9$ from IU7397)	Str ^R Kan ^S Spc ^R	This study
IU8872	D39 $\Delta cps\ \Delta bgaA::tet\text{-}P_{Zn}\text{-}RBS_{mltG}\text{-}mltG^+$ (IU1945 X fusion $\Delta bgaA::tet\text{-}P_{Zn}\text{-}RBS_{mltG}\text{-}mltG$)	Tet ^R	This study
IU8873	D39 $\Delta cps\ rpsL1\ \Delta pbp1a\ mltG(E428Q)$ (IU7325 X fusion $mltG(E428Q)$)	Str ^R Kan ^S	This study
IU8910	D39 $\Delta cps\ rpsL1\ \Delta pbp1a\ mltG(\Delta DUF_1346)$ (IU7325 X fusion $mltG(\Delta DUF_1346)$)	Str ^R Kan ^S	This study

IU8964	D39 $\Delta cps\ rpsL1\ \Delta pbp1a\ mltG(E428Q)$ $\Delta pbp2b<>aad9$ (IU8873 X $\Delta pbp2b<>aad9$ from IU7397)	Str ^R Kan ^S Spc ^R	This study
IU8980	D39 $\Delta cps\ rpsL1\ P_c-[kan-rpsL^+]-mltG^+$ (IU1824 X fusion $P_c-[kan-rpsL^+]-mltG^+$)	Kan ^R Str ^S	This study
IU8982	D39 $\Delta cps\ rpsL1\ \Delta pbp1a\ mltG(E428A)$ (IU7325 X fusion $mltG(E428A)$)	Str ^R Kan ^S	This study
IU8986	D39 $\Delta cps\ rpsL1\ mltG^+-P_c-[kan-rpsL^+]$ (IU1824 X fusion $mltG^+-P_c-[kan-rpsL^+]$)	Kan ^R Str ^S	This study
IU9025	D39 $\Delta cps\ rpsL1\ mltG(\Delta DUF_1346)$ $pbp1a^+$ (IU8980 X $mltG(\Delta DUF_1346)$ from IU8910)	Str ^R Kan ^S	This study
IU9041	D39 $\Delta cps\ rpsL1\ \Delta pbp1a\ mltG(E428Q)$ -FLAG- $P_c\text{-}erm$ (IU7325 X fusion $mltG(E428Q)$ -FLAG- $P_c\text{-}erm$)	Erm ^R Str ^R	This study
IU9043	D39 $\Delta cps\ rpsL1\ \Delta pbp1a\ mltG$ -FLAG- $P_c\text{-}erm$ (IU7325 X $mltG$ -FLAG- $P_c\text{-}erm$ from IU7403)	Erm ^R Str ^R	This study
IU9100	D39 $\Delta cps\ \Delta mltG::P_c\text{-}erm//\Delta bgaA::tet\text{-}P_{Zn}\text{-}RBS_{mltG}\text{-}mltG^+$ (IU8872 X $\Delta mltG::P_c\text{-}erm$ from IU7260)	Tet ^R Erm ^R	This study
IU9102	D39 $\Delta cps\ \Delta mltG::P_c\text{-}aad9//\Delta bgaA::tet\text{-}P_{Zn}\text{-}RBS_{mltG}\text{-}mltG^+$ (IU8872 X fusion $\Delta mltG::P_c\text{-}aad9$)	Tet ^R Spc ^R	This study
IU9148	D39 $\Delta cps\ rpsL1\ ftsZ\text{-}L_2\text{-}mKate2$ (IU7614 X fusion $ftsZ\text{-}L_2\text{-}mKate2$)	Str ^R Kan ^S	This study
IU9231	D39 $\Delta cps\ rpsL1\ \Delta walK::P_c-[kan-rpsL^+]$ (IU1824 X $\Delta walK::P_c-[kan-rpsL^+]$ from K208)	Kan ^R Str ^S	This study
IU9233	D39 $\Delta cps\ rpsL1\ \Delta pbp1a\ \Delta walK::P_c\text{-}[kan-rpsL^+]$ (IU6741 X $\Delta walK::P_c\text{-}[kan-rpsL^+]$ from K208)	Kan ^R Str ^S	This study
IU9235	D39 $\Delta cps\ rpsL1\ \Delta pbp1a\ \Delta mltG::P_c\text{-}erm$ $\Delta walK::P_c\text{-}[kan-rpsL^+]$ (IU7327 X $\Delta walK::P_c\text{-}[kan-rpsL^+]$ from K208)	Kan ^R Erm ^R Str ^S	This study
IU9278	D39 $\Delta cps\ rpsL1\ \Delta pmp23::P_c\text{-}[kan-rpsL^+]$ (IU1824 X $\Delta pmp23::P_c\text{-}[kan-rpsL^+]$ from K37)	Kan ^R Str ^S	This study
IU9290	D39 $\Delta cps\ rpsL1\ \Delta pbp1a\ \Delta mltG::P_c\text{-}erm$ $\Delta pmp23::P_c\text{-}[kan-rpsL^+]$ (IU7327 X $\Delta pmp23::P_c\text{-}[kan-rpsL^+]$ from K37)	Kan ^R Str ^S	This study
IU9292	D39 $\Delta cps\ rpsL1\ \Delta pbp1a\ \Delta mltG::P_c\text{-}erm$ $\Delta spd_1874::P_c\text{-}[kan-rpsL^+]$ (IU7327 X $\Delta spd_1874::P_c\text{-}[kan-rpsL^+]$ from K57)	Kan ^R Str ^S	This study

IU9294	D39 $\Delta cps\ rpsL\ 1\ \Delta pbp\ 1a\ \Delta mltG::P_c\text{-}erm$ $\Delta lytC::P_c\text{-}[kan\text{-}rpsL^+]$ (IU7327 X $\Delta lytC::P_c\text{-}[kan\text{-}rpsL^+]$ from K5)	Kan ^R Str ^S	This study
IU9296	D39 $\Delta cps\ rpsL\ 1\ \Delta pbp\ 1a\ \Delta mltG::P_c\text{-}erm$ $\Delta spd_0873<>P_c\text{-}[kan\text{-}rpsL^+]$ (IU7327 X $\Delta spd_0873<>P_c\text{-}[kan\text{-}rpsL^+]$ from K29)	Kan ^R Str ^S	This study
IU9298	D39 $\Delta cps\ rpsL\ 1\ \Delta pbp\ 1a\ \Delta mltG::P_c\text{-}erm$ $\Delta lytB::P_c\text{-}[kan\text{-}rpsL^+]$ (IU7327 X $\Delta lytB::P_c\text{-}[kan\text{-}rpsL^+]$ from K27)	Kan ^R Str ^S	This study
IU9316	D39 $\Delta cps\ rpsL\ 1\ \Delta pbp\ 1a\ \Delta mltG::P_c\text{-}erm$ $\Delta spd_0104::P_c\text{-}[kan\text{-}rpsL^+]$ (IU7327 X $\Delta spd_0104::P_c\text{-}[kan\text{-}rpsL^+]$ from K15)	Kan ^R Str ^S	This study
IU9318	D39 $\Delta cps\ rpsL\ 1\ \Delta pbp\ 1a\ \Delta mltG::P_c\text{-}erm$ $\Delta spd_0703::P_c\text{-}[kan\text{-}rpsL^+]$ (IU7327 X $\Delta spd_0703::P_c\text{-}[kan\text{-}rpsL^+]$ from K489)	Kan ^R Str ^S	This study
IU9320	D39 $\Delta cps\ rpsL\ 1\ \Delta pbp\ 1a\ \Delta mltG::P_c\text{-}erm$ $\Delta pspA::P_c\text{-}[kan\text{-}rpsL^+]$ (IU7327 X $\Delta pspA::P_c\text{-}[kan\text{-}rpsL^+]$ from K75)	Kan ^R Str ^S	This study
IU9330	D39 $\Delta cps\ rpsL\ 1\ \Delta pbp\ 1a\ mltG(\Delta 488bp)$ $\Delta bgaA'\text{:}:kant1t2\text{-}P_{fcsK}\text{-}pcsB^+$ (IU8553 X $\Delta bgaA'\text{:}:kant1t2\text{-}P_{fcsK}\text{-}pcsB^+$ from IU2519)	Kan ^R Str ^R	This study
IU9382	D39 $\Delta cps\ rpsL\ 1\ \Delta pbp\ 1a\ \Delta mltG::P_c\text{-}erm$ $\Delta lytA::P_c\text{-}[kan\text{-}rpsL^+]$ (IU7327 X $\Delta lytA::P_c\text{-}[kan\text{-}rpsL^+]$ from K43)	Kan ^R Str ^S	This study
IU9384	D39 $\Delta cps\ rpsL\ 1\ \Delta pbp\ 1a\ \Delta mltG::P_c\text{-}erm$ $\Delta cbpD::P_c\text{-}[kan\text{-}rpsL^+]$ (IU7327 X $\Delta cbpD::P_c\text{-}[kan\text{-}rpsL^+]$ from K148)	Kan ^R Str ^S	This study
IU9386	D39 $\Delta cps\ rpsL\ 1\ \Delta pbp\ 1a\ \Delta mltG::P_c\text{-}erm$ $\Delta dacA::P_c\text{-}[kan\text{-}rpsL^+]$ (IU7327 X $\Delta dacA::P_c\text{-}[kan\text{-}rpsL^+]$ from K35)	Kan ^R Str ^S	This study
IU9388	D39 $\Delta cps\ rpsL\ 1\ \Delta pbp\ 1a\ \Delta mltG::P_c\text{-}erm$ $\Delta dacB::P_c\text{-}[kan\text{-}rpsL^+]$ (IU7327 X $\Delta dacB::P_c\text{-}[kan\text{-}rpsL^+]$ from K25)	Kan ^R Str ^S	This study
IU9390	D39 $\Delta cps\ rpsL\ 1\ \Delta pbp\ 1a\ \Delta mltG::P_c\text{-}erm$ $\Delta spd_0173::P_c\text{-}[kan\text{-}rpsL^+]$ (IU7327 X $\Delta spd_0173::P_c\text{-}[kan\text{-}rpsL^+]$ from K372)	Kan ^R Str ^S	This study
IU9445	D39 $\Delta cps\ rpsL\ 1\ \Delta pbp\ 1a\ mltG(E428A)\text{-}$ FLAG-P _c -erm (IU7325 X fusion $mltG(E428A)\text{-FLAG-P}_c\text{-erm}$)	Erm ^R Str ^R	This study
IU9759	D39 $\Delta cps\ rpsL\ 1\ \Delta pbp\ 1a::P_c\text{-}[kan\text{-}rpsL^+]$ $mltG(\Delta 5bp)$ $\Delta pbp\ 2b<>aad9$ (IU8565 X $\Delta pbp\ 1a::P_c\text{-}[kan\text{-}rpsL^+]$ from K164)	Kan ^R Str ^S Spc ^R	This study
IU9760	D39 $\Delta cps\ rpsL\ 1\ mltG(Y488D)$ (IU8986	Str ^R Kan ^S	This study

	X <i>mltG</i> (Y488D) from IU7567)		
IU9765	D39 $\Delta cps\Delta bgaA::tet-P_{Zn}-RBS_{ftsA^-}rodZ(sp_{d_2050})^+$ (IU1945 X fusion $\Delta bgaA::tet-P_{Zn}-RBS_{ftsA^-}rodZ$)	Tet ^R	This study
IU9771	D39 <i>cps</i> ⁺ $\Delta mltG::P_c erm$ (IU1690 X $\Delta mltG::P_c erm$ from E681), <i>pbp1a</i> sequenced to contain no mutation	Erm ^R	This study
IU9772	D39 <i>cps</i> ⁺ $\Delta mltG::P_c erm$ (IU1690 X $\Delta mltG::P_c erm$ from E681), second isolate, <i>pbp1a</i> sequenced to contain no mutation	Erm ^R	This study
IU9777	D39 $\Delta cps rpsL1 pbp1a^+ mltG(\Delta 5bp)$ $\Delta pbp2b<>aad9$ (IU9759 X <i>pbp1a</i> ⁺ from IU1690)	Str ^R Kan ^S Spc ^R	This study
IU9783	D39 $\Delta cps rpsL1 mltG(Y488D)$ $\Delta pbp2b<>aad9$ (IU9760 X $\Delta pbp2b<>aad9$ from IU7397)	Str ^R Kan ^S Spc ^R	This study
IU9877	D39 $\Delta cps rpsL1 \Delta pbp1a::P_c-[kan-rpsL^+]$ <i>mltG</i> ($\Delta 488bp$) $\Delta pbp2b<>aad9$ (IU8567 X $\Delta pbp1a::P_c-[kan-rpsL^+]$ from K164)	Kan ^R Str ^S Spc ^R	This study
IU9879	D39 $\Delta cps rpsL1 \Delta pbp1a::P_c-[kan-rpsL^+]$ <i>mltG</i> ($\Omega 45bp$) ² $\Delta pbp2b<>aad9$ (IU8569 X $\Delta pbp1a::P_c-[kan-rpsL^+]$ from K164)	Kan ^R Str ^S Spc ^R	This study
IU9895	D39 $\Delta cps mltG(Y488D)-P_c erm$ (IU1945 X fusion <i>mltG</i> (Y488D)- <i>P_c erm</i>)	Erm ^R	This study
IU9897	D39 <i>cps</i> ⁺ $\Delta mltG::P_c erm$ $\Delta pbp2b<>aad9$ (IU9711 X $\Delta pbp2b<>aad9$ from IU7397)	Erm ^R Spc ^R	This study
IU9899	D39 <i>cps</i> ⁺ $\Delta mltG::P_c erm$ $\Delta cps2E::P_c-[kan-rpsL^+]$ <i>pbp1a</i> ($\Delta T@F33$) (IU9771 X $\Delta cps2E::P_c-[kan-rpsL^+]$ from IU3286), <i>pbp1a</i> sequenced to acquire a spontaneous $\Delta T@F33$ mutation	Erm ^R Kan ^R	This study
IU9905	D39 $\Delta cps rpsL1 pbp1a^+ mltG(\Delta 488bp)$ $\Delta pbp2b<>aad9$ (IU9877 X <i>pbp1a</i> ⁺ from IU1690)	Str ^R Kan ^S Spc ^R	This study
IU9907	D39 $\Delta cps rpsL1 pbp1a^+ mltG(\Omega 45bp)^2$ $\Delta pbp2b<>aad9$ (IU9879 X <i>pbp1a</i> ⁺ from IU1690)	Str ^R Kan ^S Spc ^R	This study
IU9931	D39 Δcps $\Delta rodZ(sp_{d_2050})<>aad9//\Delta bgaA::tet-P_{Zn}-RBS_{ftsA^-}rodZ^+$ (IU9765 X fusion $\Delta rodZ<>aad9$)	Tet ^R Spc ^R	This study
IU10021	D39 <i>cps</i> ⁺ $\Delta mltG::P_c erm$ $\Delta pbp1a::P_c-$	Erm ^R	This study

	[kan-rpsL ⁺](IU9711 X Δpbp1a::P _c -[kan-rpsL ⁺] from K164))	Kan ^R	
IU10048	D39 cps ⁺ ΔmltG::P _c -erm Δcps2E:: P _c -[kan-rpsL ⁺] pbp1a(G559stop) (IU9771 X Δcps2E:: P _c -[kan-rpsL ⁺] from IU3286), pbp1a sequenced to acquire a G559stop (GGA→TGA) mutation	Erm ^R Kan ^R	This study
IU10228	D39 Δcps rpsL1 gfp-L ₁ -mltG (IU8980 X fusion gfp-L ₁ -mltG)	Str ^R Kan ^S	This study
IU10292	D39 Δcps rpsL1 Δpbp1a ΔmltG::P _c -erm Δspd_1874::P _c -[kan-rpsL ⁺] Δspd_0104::P _c -cat (IU9292 X fusion Δspd_0104::P _c -cat)	Kan ^R Str ^S Cm ^R	This study
IU10294	D39 Δcps rpsL1 Δpbp1a ΔmltG::P _c -erm Δspd_0104::P _c -[kan-rpsL ⁺] Δspd_1874::P _c -cat (IU9316 X fusion Δspd_1874::P _c -cat)	Kan ^R Str ^S Cm ^R	This study
IU10318	D39 Δcps rpsL1 gfp-L ₁ -mltG ftsZ ⁺ -P _c -[kan-rpsL ⁺] (IU10228 X ftsZ ⁺ -P _c -[kan-rpsL ⁺] from IU7614)	Kan ^R Str ^S	This study
IU10320	D39 Δcps rpsL1 Δpbp1a mltG(Δ5bp)-FLAG-P _c -erm (IU7325 X fusion mltG(Δ45bp) ² -FLAG-P _c -erm)	Erm ^R Str ^R	This study
IU10323	D39 Δcps rpsL1 Δpbp1a mltG(Y488D)-FLAG-P _c -erm (IU7325 X fusion mltG(Y488D)-FLAG-P _c -erm)	Erm ^R Str ^R	This study
IU10324	D39 Δcps rpsL1 Δpbp1a mltG(Δ488bp)-FLAG-P _c -erm (IU7325 X fusion mltG(Δ488bp)-FLAG-P _c -erm)	Erm ^R Str ^R	This study
IU10327	D39 Δcps rpsL1 Δpbp1a mltG(Ω45bp) ² -FLAG-P _c -erm (IU7325 X fusion mltG(Ω45bp) ² -FLAG-P _c -erm)	Erm ^R Str ^R	This study
IU10342	D39 Δcps rpsL1 mltG(E428Q) (IU8986 X mltG(E428Q) from IU8873. This strain was sequenced to be pbp1a ⁺ , but grew poorly and was genetically unstable	Str ^R Kan ^S	This study
IU10353	D39 Δcps rpsL1 gfp-L ₁ -mltG ftsZ-L ₂ -mKate2 (IU10318 X ftsZ-L ₂ -mKate2 from IU9148)	Str ^R Kan ^S	This study
IU10369	D39 Δcps pbp1a ⁺ mltG(Y488D)-FLAG-P _c -erm (IU1945 X mltG(Y488D)-FLAG-P _c -erm from IU10323), pbp1a was sequence-confirmed to be pbp1a ⁺	Erm ^R	This study
IU10628	D39 Δcps Δpbp1a	Str ^R Kan ^S	This study

	$\Delta rodZ(sp\text{d}_2050)\text{<>}aad9$ (IU6741 X $\Delta rodZ\text{<>}aad9$ from IU9931)	Spc ^R	
IU10651	D39 $\Delta cps pbp1a^+ mltG(Y488D)$ $\Delta mreCD\text{<>}aad9$ (IU9760 X $\Delta mreCD\text{<>}aad9$ from IU1751), $pbp1a$ was sequence-confirmed to be $pbp1a^+$	Str ^R Kan ^S Spc ^R	This study
IU10656	D39 $\Delta cps pbp1a^+ mltG(Y488D)$ $\Delta rodZ(sp\text{d}_2050)\text{<>}aad9$ (IU9760 X $\Delta rodZ\text{<>}aad9$ from IU9931), $pbp1a$ was sequence-confirmed to be $pbp1a^+$	Str ^R Kan ^S Spc ^R	This study
IU10731	D39 $\Delta cps rpsL1 \Delta pbp1a mltG(\Delta 488bp)$ $\Delta mreCD\text{<>}P_c\text{-}erm$ (IU8553 X $\Delta mreCD\text{<>}P_c\text{-}erm$ from IU3897)	Str ^R Kan ^S Erm ^R	This study
IU10743	D39 $\Delta cps rpsL1 \Delta pbp1a mltG(\Delta 488bp)$ $\Delta pbp2b\text{<>}aad9 \Delta mreCD\text{<>} P_c\text{-}erm$ (IU8567 X $\Delta mreCD\text{<>} P_c\text{-}erm$ from IU3897)	Str ^R Kan ^S Spc ^R Erm ^R	This study
IU10783	D39 $\Delta cps rpsL1 mltG(Y488D)$ $\Delta pbp2b\text{<>}aad9 \Delta rodZ(sp\text{d}_2050)::P_c\text{-}[kan\text{-}rpsL^+]$ (IU9783 X $\Delta rodZ::P_c\text{-}[kan\text{-}rpsL^+]$ from K654)	Str ^R Spc ^R Kan ^R	This study
IU10785	D39 $\Delta cps rpsL1 \Delta pbp1a mltG(\Delta 488bp)$ $\Delta mreCD\text{<>}P_c\text{-}erm$ $\Delta rodZ(sp\text{d}_2050)::P_c\text{-}[kan\text{-}rpsL^+]$ (IU10731 X $\Delta rodZ::P_c\text{-}[kan\text{-}rpsL^+]$ from K654)	Str ^R Erm ^R Kan ^R	This study
IU10829	D39 $\Delta cps rpsL1 mltG(Y488D)$ $\Delta walK::P_c\text{-}[kan\text{-}rpsL^+]$ (IU9760 X $\Delta walK::P_c\text{-}[kan\text{-}rpsL^+]$ from K208)	Kan ^R Str ^S	This study
IU10919	D39 $\Delta cps rpsL1 mltG_{Spn-Eco}\text{-}P_c\text{-}erm$ (IU1824 X fusion $mltG_{Spn-Eco}\text{-}P_c\text{-}erm$)	Erm ^R	This study
IU10921	D39 $\Delta cps \Delta bgaA::tet\text{-}P_{Zn}\text{-}RBS_{rodA}\text{-}rodA^+$ (IU1945 X fusion $\Delta bgaA::tet\text{-}P_{Zn}\text{-}RBS_{rodA}\text{-}rodA$)	Tet ^R	This study
IU10943	D39 $\Delta cps rpsL1 mltG(Y488D)$ $\Delta rodA::P_c\text{-}erm$ (IU9760 X fusion $\Delta rodA::P_c\text{-}erm$)	Erm ^R	This study
IU10945	D39 $\Delta cps rpsL1 mltG(Y488D)$ $\Delta rodA::P_c\text{-}[kan\text{-}rpsL^+]$ (IU9760 X fusion $\Delta rodA::P_c\text{-}[kan\text{-}rpsL^+]$)	Kan ^R	This study
IU10965	D39 $\Delta cps rpsL1 \Delta pbp1a mltG_{Spn-Eco}\text{-}P_c\text{-}erm$ (IU6741 X $mltG_{Spn-Eco}\text{-}P_c\text{-}erm$ from IU10919)	Str ^R Kan ^S Erm ^R	This study
IU11007	D39 $\Delta cps rpsL1 mltG_{Eco}\text{-}P_c\text{-}erm$	Erm ^R	This study

	(IU1824 X fusion <i>mltG_{Eco}-P_c-erm</i>)		
IU11009	D39 $\Delta cps\ rpsL\ 1\ \Delta pbp\ 1a\ mltG_{Eco}\text{-}P_c\text{-}erm$ (IU6741 X fusion <i>mltG_{Eco}-P_c-erm</i>)	Erm ^R	This study
E177	D39 $\Delta cps\ \Delta pbp\ 1a\text{:P}_c\text{-erm}$	Erm ^R	Land <i>et al.</i> , 2013
E193	D39 $\Delta cps\ \Delta pbp\ 1b\text{:P}_c\text{-erm}$	Erm ^R	Land & Winkler, 2011
E655	D39 $\Delta cps\ \Delta rodZ(spd_2050)\text{:P}_c\text{-erm}$, (likely has suppressor) (IU1945 X fusion $\Delta rodZ\text{:P}_c\text{-erm}$)	Erm ^R	This study
E681	D39 $\Delta cps\ \Delta mltG\text{:P}_c\text{-erm}$ (IU1945 X fusion $\Delta mltG\text{:P}_c\text{-erm}$)	Erm ^R	This study
K5	D39 $\Delta cps\ \Delta lytC\text{:P}_c\text{-}[kan-rpsL^+]$ (IU1945 X fusion $\Delta lytC\text{:P}_c\text{-}[kan-rpsL^+]$)	Kan ^R	This study
K15	D39 $\Delta cps\ \Delta spd_0104\text{:P}_c\text{-}[kan-rpsL^+]$ (IU1945 X fusion $\Delta spd_0104\text{:P}_c\text{-}[kan-$ $rpsL^+]$)	Kan ^R	This study
K25	D39 $\Delta cps\ \Delta dacB\text{:P}_c\text{-}[kan-rpsL^+]$ (IU1945 X fusion $\Delta dacB\text{:P}_c\text{-}[kan-rpsL^+]$)	Kan ^R	This study
K27	D39 $\Delta cps\ \Delta lytB<>P_c\text{-}[kan-rpsL^+]$ (Regrowth of IU3877)	Kan ^R	This study
K29	D39 $\Delta cps\ \Delta spd_0873\text{:P}_c\text{-}[kan-rpsL^+]$ (Regrowth of IU3878)	Kan ^R	This study
K35	D39 $\Delta cps\ \Delta dacA\text{:P}_c\text{-}[kan-rpsL^+]$ (IU1945 X fusion $\Delta dacA\text{:P}_c\text{-}[kan-rpsL^+]$)	Kan ^R	This study
K37	D39 $\Delta cps\ \Delta pmp23\text{:P}_c\text{-}[kan-rpsL^+]$ (IU1945 X fusion $\Delta pmp23\text{:P}_c\text{-}[kan-$ $rpsL^+]$)	Kan ^R	This study
K43	D39 $\Delta cps\ \Delta lytA\text{:P}_c\text{-}[kan-rpsL^+]$ (IU1945 X fusion $\Delta lytA\text{:P}_c\text{-}[kan-rpsL^+]$)	Kan ^R	This study
K57	D39 $\Delta cps\ \Delta spd_1874\text{:P}_c\text{-}[kan-rpsL^+]$ (IU1945 X fusion $\Delta spd_1874\text{:P}_c\text{-}[kan-$ $rpsL^+]$)	Kan ^R	This study
K75	D39 $\Delta cps\ \Delta pspA\text{:P}_c\text{-}[kan-rpsL^+]$ (IU1945 X fusion $\Delta pspA\text{:P}_c\text{-}[kan-rpsL^+]$)	Kan ^R	This study
K148	D39 $\Delta cps\ \Delta cbpD\text{:P}_c\text{-}[kan-rpsL^+]$ (IU1945 X fusion $\Delta cbpD\text{:P}_c\text{-}[kan-$ $rpsL^+]$)	Kan ^R	This study
K164	D39 $\Delta cps\ \Delta pbp\ 1a\text{:P}_c\text{-}[kan-rpsL^+]$ (IU1945 transformed with fusion $\Delta pbp\ 1a\text{:P}_c\text{-}[kan-rpsL^+]$)	Kan ^R	This study
K166	D39 $\Delta cps\ \Delta pbp\ 2a\text{:P}_c\text{-}[kan-rpsL^+]$ (IU1945 X fusion $\Delta pbp\ 2a\text{:P}_c\text{-}[kan-$ $rpsL^+]$)	Kan ^R	This study
K180	D39 $\Delta cps\ \Delta pbp\ 1b\text{:P}_c\text{-}[kan-rpsL^+]$	Kan ^R	Tsui <i>et al.</i> , 2014

K208	D39 Δ cps Δ walK::P _c -[kan-rpsL ⁺](IU1945 X fusion Δ walK::P _c -[kan-rpsL ⁺])	Kan ^R	This study
K372	D39 Δ cps Δ spd_0173::P _c -[kan-rpsL ⁺](IU1945 X fusion Δ spd_0173::P _c -[kan-rpsL ⁺])	Kan ^R	This study
K489	D39 Δ cps Δ spd_0703::P _c -[kan-rpsL ⁺] (IU1945 X fusion Δ spd_0703::P _c -[kan-rpsL ⁺])	Kan ^R	This study
K637	D39 Δ cps Δ mItG::P _c -[kan-rpsL ⁺] (IU1945 X fusion Δ mItG::P _c -[kan-rpsL ⁺])	Kan ^R	This study
K654	D39 Δ cps Δ rodZ(spd_2050)::P _c -[kan-rpsL ⁺] (likely has suppressor) (IU1945 X fusion Δ rodZ::P _c -[kan-rpsL ⁺])	Kan ^R	This study

304

305

^aStrains were constructed as described in *Experimental procedures and above*.

306

307

^bPrimers used to synthesize fusion amplicons are listed in Table S2. FLAG-tagged (FLAG), c-Myc-tagged (Myc), and HA-tagged (HA) fusions were made to the carboxyl-end of MltG. The amino acid sequences of the FLAG, Myc, and HA epitope tags are DYKDDDDK (Hopp *et al.*, 1988, Wayne *et al.*, 2010), EQKLISEEDL (Evan *et al.*, 1985), and YPYDVPDYA (Wilson *et al.*, 1984), respectively. FLAG³ indicates three tandem sequences of the FLAG epitope, and L in *mreC-L-FLAG*³ refers to a 10-amino-acid spacer linker (GSAGSAAGSG) (Waldo *et al.*, 1999; Wayne *et al.*, 2010)). L₁ linker sequence in *gfp-L₁-mItG* is LEGSG (Fleurie *et al.*, 2014). The DNA template for *gfp* is pUC57-*gfp(Sp)* (Martin *et al.*, 2010), which was codon optimized for *S. pneumoniae* and contains aa substitution (A206K) to prevent GFP dimerization. L₂-linker sequence in *ftsZ-L₂-mKate2* is KLDIEFLQ (Fleurie *et al.*, 2014). mKate2 is a far red monomeric fluorescent protein with codon optimized for *S. pneumoniae* (Beilharz *et al.*, 2015).

318

^cAntibiotic resistance markers: Erm^R, erythromycin; Kan^R, kanamycin; Spc^R, spectinomycin; Str^R, streptomycin; Cm^R, chloramphenicol; Tet^R, tetracycline.

320

TABLE S2. Oligonucleotide primers used in this study (order follows Table S1)

Primer	Sequence (5' to 3')	Template ^a	Amplicon Product
For construction of IU6741 ($\Delta pbp1a$)			
P234	CCCTTGTGTTCATAGCGAGGATAAGCA	D39	5' upstream fragment with 60 bp of 5' <i>pbp1a</i>
SV022	TCAGGGGTTGTATTTGATTGTTGCAAGCTTAAGAAGCTA ATGCTCAGATACTTG		
SV023	CTGAGCATTAGCTTCTTAAGCTTGCAACAAATCAAATACA ACCCCTGATCAA	D39	60 bp of 3' <i>pbp1a</i> and 3' downstream fragment
P235	AGGCAAGCCTGCAACCATGGTCTTGAAA		
For construction of IU7399 (<i>mltG-HA-P_c-kan</i>)			
TT507	TCAGCAGGTGGTTACTTGGTTACCAAGTACG	D39	5' <i>mltG</i> ⁺ flanking fragment
TT519	GGTTAACATAATCTGGAACATCATATGGATAGTTAAT TTGCTGTTGACATGTTCAGCG		
TT520	CGCTAACATGTCAACAGCAAATTAAACTATCCATATGA TGTTCCAGATTATGCTTAACC	IU6929 ^b	HA-P _c -kan
TT517	ACATAATTTAGTTGTTACTAAAACAATTCCATCCAGTA AAATATAATATTTATTTTC		
TT518	TTACTGGATGAATTGTTTAGTAAACAAACTAAAATTATG TGATACTTCACATAATTTTC	D39	Intergenic between <i>mltG</i> and <i>greA</i> , and <i>greA</i>
TT508	GAGCAAACTAGGAAACTAGCCGCAGGTTG		
For construction of IU7403 (<i>mltG-FLAG-P_c-erm</i>)			
TT507	TCAGCAGGTGGTTACTTGGTTACCAAGTACG	D39	5' <i>mltG</i> ⁺ flanking fragment
TT509	CGGTTATTTATCATCATCATCTTATAATCGTTAATTG CTGTTGACATGTTCAGCG		
TT510	TGAACATGTCAACAGCAAATTAAACGATTATAAGATGA TGATGATAATAACCGGG	IU6565 ^c	FLAG-P _c -erm
TT511	AGTATCACATAATTTAGTTGTTATTCCTCCCGTTAA ATAATAGATAACTATTTAAA		
TT512	ATTATTTAACGGGAGGAATAACAAACTAAAATTATGT GATACTTCACATAATTTCTT	D39	Intergenic between <i>mltG</i> and <i>greA</i> , and <i>greA</i>
TT508	GAGCAAACTAGGAAACTAGCCGCAGGTTG		
For construction of IU7405 (<i>mltG-Myc-P_c-kan</i>)			
TT507	TCAGCAGGTGGTTACTTGGTTACCAAGTACG	D39	5' <i>mltG</i> ⁺ flanking fragment
TT515	GATCTTCTTCAGAAATAAGTTTTGTTCGTTAATTGCT GTTGACATGTTCAGCG		
TT516	TGAACATGTCAACAGCAAATTAAACGAACAAAAACTTAT TTCTGAAGAAGATCTTAACC	IU6962 ^d	Myc-P _c -kan
TT517	ACATAATTTAGTTGTTACTAAAACAATTCCATCCAGTA AAATATAATATTTATTTTC		
TT518	TTACTGGATGAATTGTTTAGTAAACAAACTAAAATTATG TGATACTTCACATAATTTTC	D39	Intergenic between <i>mltG</i> and <i>greA</i> , and <i>greA</i>
TT508	GAGCAAACTAGGAAACTAGCCGCAGGTTG		

For construction of IU7614 (<i>ftsZ</i> ⁺ -P _c -[<i>kan-rpsL</i> ⁺])			
TT165	AGTGGTGCCGATATGGCTTCATCACTGCT	D39	<i>ftsZ</i> ⁺
TT583	CATTATCCATTAATAACAAACGGATCCTATTAAACGATT TTGAAAAATGGAGGTGTATC		
Kan rpsL forward	TAGGATCCGTTGATTTTAATGGATAATG	P _c -[<i>kan-rpsL</i> ⁺] cassette ^e	P _c -[<i>kan-rpsL</i> ⁺]
Kan rpsL reverse	GGGCCCTTCCTTATGCTTTG		
TT584	CAAAGCATAAGGAAAGGGGCCGCCAATTCACAA GATGAAGATG	D39	60 bp of 3' <i>ftsZ</i> - <i>ylmE</i> ⁺
TT166	TCATTGGGAGAGCCGGTCTGTGAAGAAT		
For construction of IU8872 ($\Delta bgaA::tet$ -P _{czcD} -RBS _{mItG} -mItG)			
TT657	CGCCCCAAGTTCATCACCAATGACATCAAC	pJWV25 ^f	5' <i>bgaA</i> ':: <i>tet</i> -P _{czcD} -
TT681	AGTTTTCCCTCTGTTGATAATTGTTATAATAGATT TGAACACCTGTTCAATTATC		
TT682	ACAAGGTGTTCATAAATCTATTATAACAAATTATCAACAA GGAGGAAAAACTTTGAGTG	D39	RBS(_{mItG})- <i>mItG</i>
TT679	CAACTGGTTATGAGAAAGTAAGTTCTTTAGTTAATT GCTGTTGACATGTTCAGC		
TT680	GAACATGTCAACACGAAATTAAACTAAAAGAACTTACTT TCTCATAAACCAAGTTGCTG	D39	3' <i>bgaA</i> ' flanking
CS121	GCTTCTTGAGGCAATTCACTGGTGC		
For construction of IU8873 (mItG(E428Q))			
P1348	TCTTCTTGAGCCTTGAAAGAGGTGGCAGT	D39	<i>spd_1347-5'</i> <i>mItG</i> fragment with <i>mItG</i> (E428Q)(GA A to CAA)
TT706	TCTGTCTTGGCACCTGTTTCGACCAAGGAAGCAATG G		
TT707	CTTGGTCGAAAACAAGGTGCCAAGACAGAAGATCGTA AG	D39	3' <i>mItG</i> fragment with <i>mItG</i> (E428Q)(GA A to CAA)- <i>greA</i>
P1349	AGAGCAAACCTAGGAAACTAGCCGCAGGTTG		
For construction of IU8910 (mItG(Δ DUF_1346))			
P1348	TCTTCTTGAGCCTTGAAAGAGGTGGCAGT	D39	5' upstream fragment with 98 bp of 5' <i>mItG</i>
TT708	CGTGATGTATCTGATGATATCCACTACTTTCTAAAT CTCTCAGAACATCTGCTCTT		
TT709	GCAGATTCTGAGAGATTAGAAAAAGTAGTGGATATCAT CAGAGATACATCACGTG	D39	1213 bp of 3' <i>mItG</i> and 3' downstream fragment
P1349	AGAGCAAACCTAGGAAACTAGCCGCAGGTTG		
For construction of IU8980 (P _c -[<i>kan-rpsL</i> ⁺]-mItG ⁺)			
P1348	TCTTCTTGAGCCTTGAAAGAGGTGGCAGT	D39	<i>spd_1347</i> ⁺
TT730	CATTATCCATTAATAACAAACGGATCCTATTATTTTC ATTTCCCAGACCATATCATA		
Kan rpsL forward	TAGGATCCGTTGATTTTAATGGATAATG	P _c -[<i>kan-rpsL</i> ⁺] cassette ^e	P _c -[<i>kan-rpsL</i> ⁺]
Kan rpsL reverse	GGGCCCTTCCTTATGCTTTG		

TT731	CAAAAGCATAAGGAAAGGGGCCGTAGGAAAAGTATC ATAGATTGCTTTTTGGACTT	D39	80 bp upstream of <i>mltG</i> and 5' of <i>mltG</i> ⁺
TT412	CGACCAAGGAAGCAATGGTCAACAACTCAT		
For construction of IU8982 (<i>mltG</i>(E428A))			
P1348	TCTTCTGCAGCCTTGAAAGAGGTGGCAGT	D39	<i>spd_1347</i> ⁺ -5' <i>mltG</i> fragment with <i>mltG</i> (E428A)(GA A to GCA)
TT728	TCTGTCTGGCACCTGCTTTTCGACCAAGGAAGCAAT GG		
TT729	CTTGGTCGAAAAGCAGGTGCCAAGACAGAACAGATCGTA AG	D39	3' <i>mltG</i> fragment with <i>mltG</i> (E428A)(GA A to GCA)- <i>greA</i>
P1349	AGAGCAAACTAGGAAACTAGCCGCAGGTTG		
For construction of IU8986 (<i>mltG</i>⁺-P_c-[kan-rpsL⁺])			
TT415	AAGCAGAACAGCAGGTCCAGAACACCTACG	D39	3' <i>mltG</i>
TT726	CATTATCCATTAAAAATCAAACGGATCCTATTAGTTAAT TTGCTGTTGACATGTTCAGC		
Kan rpsL forward	TAGGATCCGTTGATTTTAATGGATAATG	P _c -[kan-rpsL ⁺] cassette ^e	P _c -[kan-rpsL ⁺]
Kan rpsL reverse	GGGCCCCTTCCCTATGCTTTG		
TT727	CAAAAGCATAAGGAAAGGGGCCACAAACTAAAATTAT GTGATACTTCACATAATTTCT	D39	Intergenic between <i>mltG</i> and <i>greA</i> , and <i>greA</i>
P1349	AGAGCAAACTAGGAAACTAGCCGCAGGTTG		
For construction of IU9041 (<i>mltG</i>(E428Q)-FLAG-P_c-erm)			
P1348	TCTTCTGCAGCCTTGAAAGAGGTGGCAGT	D39	<i>spd_1347</i> -5' <i>mltG</i> fragment with <i>mltG</i> (E428Q)(GA A to CAA)
TT706	TCTGTCTGGCACCTGTTTCGACCAAGGAAGCAATG G		
TT707	CTTGGTCGAAAACAAGGTGCCAAGACAGAACAGATCGTA AG	IU7403 ^g	3' <i>mltG</i> fragment with <i>mltG</i> (E428Q)- FLAG-P _c -erm- <i>greA</i>
P1349	AGAGCAAACTAGGAAACTAGCCGCAGGTTG		
For construction of IU9102 (Δ<i>mltG</i>::P_c-aad9)			
P1348	TCTTCTGCAGCCTTGAAAGAGGTGGCAGT	E681 ^g	5' upstream fragment with 90 bp of 5' <i>mltG</i> and P _c
TT688	GTATTCAAATATATCCTCCTCATTATTATTCCTCCTC TTTCTACAGTATTAAAGA		
TT689	ACTGTAGAAAAGAGGAAGGAAATAATAATGAGGAGGA TATATTGAATACATACGAACA	IU7397 ^g	aad9
TT690	TTTAGTACCGTATTATAATTTTTAATCTGTTATTAAAT AGTTTATAGTTAAATTAC		
TT691	CTATTTAAATAACAGATTAATATAATACGGTACT AAACGTCCAAAAGCATAAGG	E681 ^g	90 bp of 3' <i>mltG</i> and 3' downstream fragment
P1349	AGAGCAAACTAGGAAACTAGCCGCAGGTTG		

For construction of IU9148 (<i>ftsZ</i>-L₂-<i>mKate2</i>)			
TT165	AGTGGTGCCGATATGGCTTCATCACTGCT	IU8845 ^h	3' <i>ftsZ</i> -L ₂
TT746	TGTGCATATTTCTTGTATAAGTTCTGACATCTGCAGGA ACTCGATGTCTAGTTACG		
TT747	AAACTAGACATCGAGTCTGCAGATGTCAGAACTTATC AAGGAAAATATGCACA	pKB01_mK ate2 ⁱ	<i>mKate2</i>
TT748	TTAACGGTGTCCAATTACTAGGCCAATCAC		
TT749	TTGCCTAGTAAATTGGGACACCGTTAACATTTCAAAA ATCGTTAAGTAAATGAATGTA	D39	17 bp of 3' <i>ftsZ</i> - <i>ylmE</i> ^j
TT166	TCATTGGGAGAGCCGGTCTGTGAAGAAT		
For construction of IU9445 (<i>mltG</i>(E428A)-FLAG-P_c-erm)			
P1348	TCTTCTTGCAGCCTTGAAAGAGGTGGCAGT	D39	<i>spd_1347-5'</i> <i>mltG</i> fragment with <i>mltG</i> (E428A)
TT728	TCTGTCTGGCACCTGCTTTTCGACCAAGGAAGCAAT GG		
TT729	CTTGGTCGAAAAGCAGGTGCCAAGACAGAAGATCGTA AG	IU7403 ^g	3' <i>mltG</i> fragment with <i>mltG</i> (E428A)- FLAG-P _c -erm- <i>greA</i>
P1349	AGAGCAAACTAGGAAACTAGCCGCAGGTTG		
For construction of IU9765 ($\Delta bgaA::tet\text{-}P_{Zn}\text{-RBS}_{ftsA}\text{-rodZ}(spd_2050)^+$)			
TT657	CGCCCCAAGTTCATCACCAATGACATCAAC	IU8906 ^l	5' <i>bgaA'::tet\text{-}P_{czCD}</i> -RBS _{ftsA}
TT769	CCTCTCAATTGTTTTTTCTCATTACATCGCTTCTCT CTATCTCCTTGT		
TT770	GGAAGATAGAGAGGAAGCGATGTAATGAGAAAAAAAAC AATTGGAGAGGTTTAC	D39	<i>rodZ</i>
TT771	ACTGGTTATGAGAAAGTAAGTTCTTTAATTTTAGTAA AGGTTACAGTGATTGTCCA		
TT772	AAATCACTGTAACCTTACTAAAAATTAAAAGAACTTACT TTCTCATAAACCAGTTGCTG	D39	3' <i>bgaA'</i> flanking
CS121	GCTTCTTGAGGCAATTCACTTGGTGC		
For construction of IU9895 (<i>mltG</i>(Y488D)-P_c-erm)			
P1348	TCTTCTTGCAGCCTTGAAAGAGGTGGCAGT	IU7567 ^g	upstream of <i>mltG</i> and <i>mltG</i> (Y488D)
TT726	CATTATCCATTAAAAATCAAACGGATCCTATTAGTTAAT TTGCTGTTGACATGTTCA		
Kan rpsL forward	TAGGATCCGTTGATTTAATGGATAATG	P _c -erm cassette ^e	P _c -erm
Kan rpsL reverse	GGGCCCTTCCTTATGCTTTG		
TT727	CAAAGCATAAGGAAAGGGGCCACAAACTAAAATTAT GTGATACTTCACATAATTTCT	D39	Intergenic between <i>mltG</i> and <i>greA</i> , and <i>greA</i>
P1349	AGAGCAAACTAGGAAACTAGCCGCAGGTTG		
For construction of IU9931 ($\Delta rodZ(spd_2050)\text{<gt;aad9}$)			
P1384	GAGGTAAGCGAGAAGTTCTGAAGCGGATTGC	D39	5' upstream fragment
TT311	GTATGTATTCAAATATATCCTCCTCACACTTGTCTATTATG		

TT312	GACACTAGAAGAAGGGATGACAAGTGTGAGGAGGATA TATTGAAATACATACGAACA	IU7397 ^g	<i>aad9</i>
TT313	CTTTTTTCATTCGTTTCCCTATAATTTTTAATCTGTT ATTTAAATAGTTATAGTT		
TT314	CTATTTAAATAACAGATTAACAAAAATTATAAGGAAAACG AATGAAAAAAAGAACAAATC	D39	3' downstream fragment
P1385	ACAAACACCTGCAATGCCACACGTTGCTT		

For construction of IU10228 (*gfp-L₁-mltG*)

P1348	TCTTCTTGCAGCCTTGAAAGAGGTGGCAGT	D39	<i>spd_1347</i>
TT854	TAAACAATTCTCACCTTAGAAATCATAAGTTTCCCTC CTTGTGATAATCC		
TT855	ATCAACAAGGAGGAAAAACTTATGATTCTAAAGGTGAA GAATTGTTACAGGTGT	IU9020 ^l	<i>gfp-L₁</i> with ATG start codon
TT757	TCCGGATCCCTCGAGTTATACAATTATCC		
TT853	GAATTGTATAAACCTCGAGGGATCCGGAAAGTGAAAAGTC AAGAGAAGAGAGAAATTAGC	D39	5' <i>mltG</i> starting from second codon of <i>mltG</i>
TT412	CGACCAAGGAAGCAATGGTCAACAACCATCAT		

For construction of IU10292 (Δ *spd_0104::P_c-cat*)

P108	ACGAGTGACATTCTGGCGAT	K15 ^g	5' upstream fragment with 60 bp of 5' <i>spd_0104-P_c</i>
MB12	AAATCAATTATTAAAGTTTACATTATTATTTCCCTCCTCT TTTCTACAGTATTAAAGA		
MB11	TGTAGAAAAGAGGAAGGAAATAATAATGAACCTTAATA AAATTGATTAGACAATTGGA	IU3373 ^k	<i>cat</i> ORF
TT869	GCCCCCTTCCTTATGCTTTGTTATAAAAGCCAGTCATT AGGCCTATCTGA		
TT870	AGGCCTAATGACTGGCTTTATAACAAAAGCATAAGGAA AGGGGCC	K15 ^g	60 bp of 3' <i>spd_0104</i> and 3' downstream fragment
P111	ACCACCTCATACCACTGTCTGTT		

For construction of IU10294 (Δ *spd_1874::P_c-cat*)

P174	ATGTGGTGTATCCGCATTGGGACAGGAT	K57 ^g	5' upstream fragment with 60 bp of 5' <i>spd_1874-P_c</i>
MB12	AAATCAATTATTAAAGTTTACATTATTATTTCCCTCCTCT TTTCTACAGTATTAAAGA		
MB11	TGTAGAAAAGAGGAAGGAAATAATAATGAACCTTAATA AAATTGATTAGACAATTGGA	IU3373 ^k	<i>cat</i> ORF
TT869	GCCCCCTTCCTTATGCTTTGTTATAAAAGCCAGTCATT AGGCCTATCTGA		
TT870	AGGCCTAATGACTGGCTTTATAACAAAAGCATAAGGAA AGGGGCC	K57 ^g	60 bp of 3' <i>spd_1874</i> and 3' downstream fragment
P175	AGCCGTAAGTCGCAGCACCAATCACAA		

For construction of IU10320 (*mltG*(Δ5bp)-FLAG-P_c-erm)

P1348	TCTTCTTGCAGCCTTGAAAGAGGTGGCAGT	IU7477 ^g	<i>spd_1347,</i> <i>mltG</i> (Δ5bp)
TT509	CGGTTATTTATCATCATCATCTTATAATCGTTAATTG CTGTTGACATGTTAGCG		

TT510	TGAACATGTCAACAGCAAATTAAACGATTATAAGATGA TGATGATAATAACCGGG	IU7403 ⁹	FLAG-P _c -erm, and greA
P1349	AGAGCAAACCTAGGAAACTAGCCGCAGGTTG		
For construction of IU10323 (<i>mltG(Y488D)</i>-FLAG-P_c-erm)			
P1348	TCTTCTTGCAGCCTTGAAAGAGGTGGCACT	IU7567 ⁹	spd_1347, <i>mltG(Y488D)</i>
TT509	CGGTTATTTATCATCATCATCTTATAATCGTTAACCTTG CTGTTGACATGTTCAGCG		
TT510	TGAACATGTCAACAGCAAATTAAACGATTATAAGATGA TGATGATAATAACCGGG	IU7403 ⁹	FLAG-P _c -erm, and greA
P1349	AGAGCAAACCTAGGAAACTAGCCGCAGGTTG		
For construction of IU10324 (<i>mltG(Δ488bp)</i>-FLAG-P_c-erm)			
P1348	TCTTCTTGCAGCCTTGAAAGAGGTGGCACT	IU7570 ⁹	spd_1347, <i>mltG(Δ488bp)</i>
TT509	CGGTTATTTATCATCATCATCTTATAATCGTTAACCTTG CTGTTGACATGTTCAGCG		
TT510	TGAACATGTCAACAGCAAATTAAACGATTATAAGATGA TGATGATAATAACCGGG	IU7403 ⁹	FLAG-P _c -erm, and greA
P1349	AGAGCAAACCTAGGAAACTAGCCGCAGGTTG		
For construction of IU10327 (<i>mltG(Ω45bp)</i>²-FLAG-P_c-erm)			
P1348	TCTTCTTGCAGCCTTGAAAGAGGTGGCACT	IU7765 ⁹	spd_1347, <i>mltG(Ω45bp)</i> ²
TT509	CGGTTATTTATCATCATCATCTTATAATCGTTAACCTTG CTGTTGACATGTTCAGCG		
TT510	TGAACATGTCAACAGCAAATTAAACGATTATAAGATGA TGATGATAATAACCGGG	IU7403 ⁹	FLAG-P _c -erm, and greA
P1349	AGAGCAAACCTAGGAAACTAGCCGCAGGTTG		
For construction of IU10919 (<i>mltG_{Spn-Eco}</i>-P_c-erm)			
TT413	GAGCCTGGTGGTTATATCTCTGTGACCTGT	D39	Upstream of <i>S.pn</i> <i>mltG</i> and (N) _{Spn} - aa(1-209)
TT890	GGCAAGATGGCGAACCTTCTGGTAACCAAAGTAACCAC CTGCTG		
TT891	CAGGTGGTTACTTGGTTACCAGAAGGTTGCCATCTT GCCGA	E. coli K12 genomic DNA	aa(25-341)-(C) _{Eco}
TT892	CATTATCCATTAAAATCAAACGGATCCTATTACTGC ATTTTTTCCTTAAGCA		
Kan rpsL forward	TAGGATCCGTTGATTTAATGGATAATG	IU9895 ⁹	P _c -erm- downstream <i>mltG</i>
P1349	AGAGCAAACCTAGGAAACTAGCCGCAGGTTG		
For construction of IU10921 ($\Delta bgaA::tet\text{-}P_{czcD}\text{-}RBS_{rodA\text{-}rodA}$)			
TT657	CGCCCCAAGTTCATCACCAATGACATCAAC	IU8872 ⁹	5' <i>bgaA'::tet\text{-}P_{czcD}</i> -
TT895	TGTACTAACCTTATACTTCATATTGTTATAATAGATT TGAACACCTTGTTCATTATC		
TT896	TGTCATAAAATCTATTATAACAATATGAAAGTATAAGGTT AGTACATATGAAACGTTCTC	D39	RBS(_{rodA})- <i>rodA</i>
TT897	AACTGGTTATGAGAAAGTAAGTTCTTTATTAATTGT TTAATACAACCTTTCCG		
TT898	AAAAGGTTGTATTAACCAAATTAAATAAAAGAACTTACT TTCTCATAAACCAAGTTGCTG	D39	3' <i>bgaA'</i> flanking

CS121	GCTTTCTTGGAGGCAATTCACTTGGTGC		
For construction of IU10943 ($\Delta rodA::P_c\text{-erm}$)			
P1543	CAGGCCGTACTCTCTGCCTCTTACTTCC	D39	5' upstream fragment with 81 bp of 5' <i>rodA</i>
P1545	CATTATCCATTAAAAATCAAACGGATCCTAACGCCACCAC ACCGATGACCA		
Kan rpsL forward	TAGGATCCGTTGATTTTAATGGATAATG	$P_c\text{-erm}^e$	$P_c\text{-erm}$
Kan rpsL reverse	GGGCCCTTCCTTATGCTTTG		
P1546	CAAAAGCATAAGGAAAGGGGCCCTCGATGAGTTACCAAG ACTAATCTAGCTGAA	D39	87 bp of 3' <i>rodA</i> and 3' downstream fragment
P1544	CGGGTGTCAAGCTCTGGCTTCATTTTC		
For construction of IU10945 ($\Delta rodA::P_c\text{-[kan-rpsL}^+\text{]}$)			
P1543	CAGGCCGTACTCTCTGCCTCTTACTTCC	D39	5' upstream fragment with 81 bp of 5' <i>rodA</i>
P1545	CATTATCCATTAAAAATCAAACGGATCCTAACGCCACCAC ACCGATGACCA		
Kan rpsL forward	TAGGATCCGTTGATTTTAATGGATAATG	$P_c\text{-[kan-rpsL}^+\text{]}$ cassette ^e	$P_c\text{-[kan-rpsL}^+\text{]}$
Kan rpsL reverse	GGGCCCTTCCTTATGCTTTG		
P1546	CAAAAGCATAAGGAAAGGGGCCCTCGATGAGTTACCAAG ACTAATCTAGCTGAA	D39	87 bp of 3' <i>rodA</i> and 3' downstream fragment
P1544	CGGGTGTCAAGCTCTGGCTTCATTTTC		
For construction of IU11007 and IU11009 (<i>mltG</i>_{Eco}-$P_c\text{-erm}$)			
P1348	TCTTCTTGCAGCCTTGAAAGAGGTGGCAGT	D39	Upstream of <i>S.pn</i> <i>mltG</i>
TT903	TAACAAGATTATCAATAACACTTTTCATAAGTTTTCC TCCTGTTGATAATCCATAA		
TT904	GGATTATCAACAAGGAGGAAAAACTTATGAAAAAAAGTGT TATTGATAATCTGTTATTGC	<i>E. coli</i> K12 genomic DNA	<i>E. coli</i> <i>mltG</i> ORF
TT892	CATTATCCATTAAAAATCAAACGGATCCTATTACTGCGC ATTTTTCCCTAACGA		
Kan rpsL forward	TAGGATCCGTTGATTTTAATGGATAATG	IU9895 ^g	$P_c\text{-erm}$ -downstream <i>mltG</i>
P1349	AGAGCAAACTAGGAAACTAGCCGCAGGTTG		
For construction of E655 ($\Delta rodZ(spd_2050)::P_c\text{-erm}$)			
TT329	CAACTGATATAGTTGGAAGTGAGGAGTCCATTCCC	D39	5' upstream fragment with 60 bp of 5' <i>rodZ</i>
P1386	CATTATCCATTAAAAATCAAACGGATCCTAACTCAATCC CTGATTGATTCTAGCTAATCG		
Kan rpsL forward	TAGGATCCGTTGATTTTAATGGATAATG	$P_c\text{-erm}^e$	$P_c\text{-erm}$
Kan rpsL reverse	GGGCCCTTCCTTATGCTTTG		
P1387	CAAAAGCATAAGGAAAGGGGCCGATTATCGAAATTA ACAGCTCAGACTGG	D39	60 bp of 3' <i>rodZ</i> and 3'

P1385	ACAAACACCTGCAATGGCCACACGTTGCTT		downstream fragment
For construction of E681 ($\Delta mltG::P_c\text{-erm}$)			
P1348	TCTTCTTGCAGCCTTGAAAGAGGTGGCACT	D39	5' upstream fragment with 90 bp of 5' <i>mltG</i>
P1350	CATTATCCATTAAAATCAAACGGATCCTAACTTCATC ATAGCCTTTACTTTCTAA		
Kan rpsL forward	TAGGATCCGTTGATTTTAATGGATAATG	$P_c\text{-erm}^e$	$P_c\text{-erm}$
Kan rpsL reverse	GGGCCCTTCCTTATGCTTTG		
P1351	CAAAGCATAAGGAAAGGGGCCGATGTCACAGAAGG CAAGGTCTACTATG	D39	90 bp of 3' <i>mltG</i> and 3' downstream fragment
P1349	AGAGCAAATAGGAAACTAGCCGCAGGTTG		
For construction of K5 (<math>\Delta lytC::P_c\text{-[kan-rpsL⁺⁾</math>			
P13	TTTGAGAAACTGGCGCCATGAAGG	D39	5' upstream fragment with 60 bp of 5' <i>lytC</i>
P17	CATTATCCATTAAAATCAAACGGATCCTAGACATGACT AGTTGCCAAGCCTAGTAAAC		
Kan rpsL forward	TAGGATCCGTTGATTTTAATGGATAATG	$P_c\text{-[kan-rpsL+ cassettee$	$P_c\text{-[kan-rpsL+$
Kan rpsL reverse	GGGCCCTTCCTTATGCTTTG		
P18	CAAAGCATAAGGAAAGGGGCCACCTCTTCTGAATAC ATGAAAGGAATCCA	D39	60 bp of 3' <i>lytC</i> and 3' downstream fragment
P14	AAACCAGGTGCTTGTCCAAGTTCG		
For construction of K15 (<math>\Delta spd_0104::P_c\text{-[kan-rpsL⁺⁾</math>			
P108	ACGAGTGACATTCTGGCGAT	D39	5' upstream fragment with 60 bp of 5' <i>spd_0104</i>
P120	CATTATCCATTAAAATCAAACGGATCCTATGCAAACAA GGCAGCTACTCCTG		
Kan rpsL forward	TAGGATCCGTTGATTTTAATGGATAATG	$P_c\text{-[kan-rpsL+ cassettee$	$P_c\text{-[kan-rpsL+$
Kan rpsL reverse	GGGCCCTTCCTTATGCTTTG		
P121	CAAAGCATAAGGAAAGGGGCCGGACGTTACGGTTCAATGGACTGC	D39	60 bp of 3' <i>spd_0104</i> and 3' downstream fragment
P111	ACCACCTCATCACCACTGTCTGTT		
For construction of K25 (<math>\Delta dacB::P_c\text{-[kan-rpsL⁺⁾</math>			
P136	ACTGCCCATGTAGATACGCTTGGTGCTA	D39	5' upstream fragment with 60 bp of 5' <i>dacB</i>
P140	CATTATCCATTAAAATCAAACGGATCCTATGAACACAAGCTGCTAGACTCAAGGCTAG		
Kan rpsL forward	TAGGATCCGTTGATTTTAATGGATAATG	$P_c\text{-[kan-rpsL+ cassettee$	$P_c\text{-[kan-rpsL+$
Kan rpsL reverse	GGGCCCTTCCTTATGCTTTG		
P141	CAAAGCATAAGGAAAGGGGCCGAGAGTGGTCTCAG TTTGGAAGAATACTATG	D39	60 bp of 3' <i>dacB</i> and 3'

P137	ACCGTTGGCAATACCATTGCTCCACGG		downstream fragment
For construction of K35 ($\Delta dacA::P_c-[kan-rpsL^+]$)			
P150	AGCCTGCAATATGCAAGCGATCCCTCTT	D39	5' upstream fragment with 60 bp of 5' <i>dacA</i>
P152	CATTATCCATTAAAATCAAACGGATCCTAAGCAGTAGAACACCCCCCTAAAAGAGAGAC		
Kan rpsL forward	TAGGATCCGTTGATTTTAATGGATAATG	$P_c-[kan-rpsL^+]$ cassette ^e	$P_c-[kan-rpsL^+]$
Kan rpsL reverse	GGGCCCTTCCTTATGCTTTG		
P153	CAAAGCATAAGGAAAGGGGCCCTCTTCTTAAAAGTTTGGTGAATCAGTTG	D39	60 bp of 3' <i>dacA</i> and 3' downstream fragment
P151	TATCGTTGATGAGGGAGCAAGCGTCCACTA		
For construction of K37 ($\Delta pmp23::P_c-[kan-rpsL^+]$)			
P154	AGTCAGTCGGATGATACCGAGCTGTT	D39	5' upstream fragment with 60 bp of 5' <i>pmp23</i>
P156	CATTATCCATTAAAATCAAACGGATCCTATTATAGCCAGCAAAAGGAAGACTGCTAG		
Kan rpsL forward	TAGGATCCGTTGATTTTAATGGATAATG	$P_c-[kan-rpsL^+]$ cassette ^e	$P_c-[kan-rpsL^+]$
Kan rpsL reverse	GGGCCCTTCCTTATGCTTTG		
P157	CAAAGCATAAGGAAAGGGGCCGTACGACTAACCTTACATCATCAAATGTTTC	D39	60 bp of 3' <i>pmp23</i> and 3' downstream fragment
P155	ACTGTCGCCAGCTTGTGATACGATGCTT		
For construction of K43 ($\Delta lytA::P_c-[kan-rpsL^+]$)			
P166	CCTTGCCCTTCTCCTATGACCGCTAT	D39	5' upstream fragment with 60 bp of 5' <i>lytA</i>
P168	CATTATCCATTAAAATCAAACGGATCCTAATATGGTTGCACGCCACTTGAGGC		
Kan rpsL forward	TAGGATCCGTTGATTTTAATGGATAATG	$P_c-[kan-rpsL^+]$ cassette ^e	$P_c-[kan-rpsL^+]$
Kan rpsL reverse	GGGCCCTTCCTTATGCTTTG		
P169	CAAAGCATAAGGAAAGGGGCCCTGGCAGACAGGCCAGAATTCACAGTAGAG	D39	60 bp of 3' <i>lytA</i> and 3' downstream fragment
P167	CCTCAACCACCTATACAGTGAAGATGGGA		
For construction of K57 ($\Delta spd_1874::P_c-[kan-rpsL^+]$)			
P174	ATGTGGTGTATCCGCATTGGGACAGGAT	D39	5' upstream fragment with 60 bp of 5' <i>spd_1874</i>
P176	CATTATCCATTAAAATCAAACGGATCCTATGCCAATACGGGGCAAATGACAAGGC		
Kan rpsL forward	TAGGATCCGTTGATTTTAATGGATAATG	$P_c-[kan-rpsL^+]$ cassette ^e	$P_c-[kan-rpsL^+]$
Kan rpsL reverse	GGGCCCTTCCTTATGCTTTG		
P177	CAAAGCATAAGGAAAGGGGCCCGTGGTAGTGTGACAGAAAATCACTATGATCACG	D39	60 bp of 3' <i>spd_1874</i> and 3'

P175	AGCCGTAAGTCGCAGCACCAATCACAAA		downstream fragment
For construction of K75 ($\Delta pspA::P_c-[kan-rpsL^+]$)			
P70	ACCGTTGGCAATTATGGTACATGGACA	D39	5' upstream fragment with 60 bp of 5' <i>pspA</i>
P72	CATTATCCATTAAAATCAAACGGATCCTAACAGCCCC TAAGATAGCGACGCTGGC		
Kan rpsL forward	TAGGATCCGTTGATTTTAATGGATAATG	$P_c-[kan-rpsL^+]$ cassette ^e	$P_c-[kan-rpsL^+]$
Kan rpsL reverse	GGGCCCTTCCTTATGCTTTG		
P73	CAAAGCATAAGGAAAGGGGCCCTGCAGTCAACACA ACTGTAGATGGCTAT	D39	60 bp of 3' <i>pspA</i> and 3' downstream fragment
P71	TCCTTGTTGCACATAACGTCCGGATTGGC		
For construction of K148 ($\Delta cbpD::P_c-[kan-rpsL^+]$)			
P202	TATCTTAGCAGCTCGTCCAGCAGTTGGT	D39	5' upstream fragment with 60 bp of 5' <i>cbpD</i>
P204	CATTATCCATTAAAATCAAACGGATCCTATTAACTGA CATCTCAAGTAATAACTTG		
Kan rpsL forward	TAGGATCCGTTGATTTTAATGGATAATG	$P_c-[kan-rpsL^+]$ cassette ^e	$P_c-[kan-rpsL^+]$
Kan rpsL reverse	GGGCCCTTCCTTATGCTTTG		
P205	CAAAGCATAAGGAAAGGGGCCCTAGCTATTAAATACG ACGGTGGATGGCTACAG	D39	60 bp of 3' <i>cbpD</i> and 3' downstream fragment
P203	AGCTATGGCAATGGCGGAATGGTCTGA		
For construction of K164 ($\Delta pbp1a::P_c-[kan-rpsL^+]$)			
P234	CCCTTGTGTCATAGCGAGGATAAGCA	D39	5' upstream fragment with 60 bp of 5' <i>pbp1a</i>
P236	CATTATCCATTAAAATCAAACGGATCCTACAAGCTAA GAAGCTAATGCTCAGATACTT		
Kan rpsL forward	TAGGATCCGTTGATTTTAATGGATAATG	$P_c-[kan-rpsL^+]$ cassette ^e	$P_c-[kan-rpsL^+]$
Kan rpsL reverse	GGGCCCTTCCTTATGCTTTG		
P237	CAAAGCATAAGGAAAGGGGCCCAACAATCAAATACA ACCCCTGATCAACAAAATC	D39	60 bp of 3' <i>pbp1a</i> and 3' downstream fragment
P235	AGGCAAGCCTGCAACCATGGTCTTGAAA		
For construction of K166 ($\Delta pbp2a::P_c-[kan-rpsL^+]$)			
P226	GGTACGACAACGAAATGTCATACACTGCAC	D39	5' upstream fragment with 60 bp of 5' <i>pbp2a</i>
P228	CATTATCCATTAAAATCAAACGGATCCTATTCACTTGTT TCTTTTTAAAAGAGAAAG		
Kan rpsL forward	TAGGATCCGTTGATTTTAATGGATAATG	$P_c-[kan-rpsL^+]$ cassette ^e	$P_c-[kan-rpsL^+]$
Kan rpsL reverse	GGGCCCTTCCTTATGCTTTG		
P229	CAAAGCATAAGGAAAGGGGCCCGGAAGATTAAGGA AAAGGCTCAAACAATATG	D39	60 bp of 3' <i>pbp2a</i> and 3'

P227	TCTGTTCCCGTGTGATCCGACAAATCCT		downstream fragment
For construction of K208 ($\Delta walK::P_c-[kan-rpsL^+]$)			
TT163	AGCAGTTGACCTCTTCATCAGGTTGCGG	D39	5' upstream fragment with 60 bp of 5' walK
P508	CATTATCCATTAAAATCAAACGGATCCTACAAAATCAG GATAAAGATAAAATCTCTGGT		
Kan rpsL forward	TAGGATCCGTTGATTTTAATGGATAATG	$P_c-[kan-rpsL^+]$ cassette ^e	$P_c-[kan-rpsL^+]$
Kan rpsL reverse	GGGCCCTTCCTTATGCTTTG		
P509	CAAAGCATAAGGAAAGGGGCCGTACTCCCTTATGAT AAGGATGCAGTGAAA	D39	60 bp of 3' walK and 3' downstream fragment
TT164	TGTCAATGGTGTGCGGTATCTGGTGAGGT		
For construction of K372 ($\Delta spd_0173::P_c-[kan-rpsL^+]$)			
P830	TATACGGCGCACCAACTCATTGGGCTCATA	D39	5' upstream fragment with 60 bp of 5' spd_0173
P832	CATTATCCATTAAAATCAAACGGATCCTAGACAAAATC CTCTCCGATAATGCCA		
Kan rpsL forward	TAGGATCCGTTGATTTTAATGGATAATG	$P_c-[kan-rpsL^+]$ cassette ^e	$P_c-[kan-rpsL^+]$
Kan rpsL reverse	GGGCCCTTCCTTATGCTTTG		
P833	CAAAGCATAAGGAAAGGGGCCCATGCTCATGTAGAT GCACAGGAACA	D39	60 bp of 3' spd_0173 and 3' downstream fragment
TT831	AACGCCAAGCCTTCTACAGTTACAGGCA		
For construction of K489 ($\Delta spd_0703::P_c-[kan-rpsL^+]$)			
P1063	TTTCCAGCGAGTAAAGCCATGCTCCACCAA	D39	5' upstream fragment with 60 bp of 5' spd_0703
P1065	CATTATCCATTAAAATCAAACGGATCCTACTGCTGGTT TAATTCTTCTTGATAGTCTAC		
Kan rpsL forward	TAGGATCCGTTGATTTTAATGGATAATG	$P_c-[kan-rpsL^+]$ cassette ^e	$P_c-[kan-rpsL^+]$
Kan rpsL reverse	GGGCCCTTCCTTATGCTTTG		
P1066	CAAAGCATAAGGAAAGGGGCCGTTAACGGTCTATT ATCAAACGAAACGT	D39	39 bp of 3' spd_0703 and 3' downstream fragment
P1064	CCCTGCTTGAGAGTATGCAGAAGCAACAGT		
For construction of K637 ($\Delta mltG::P_c-[kan-rpsL^+]$)			
P1348	TCTTCTTGCAGCCTTGAAAGAGGTGGCAGT	D39	5' upstream fragment with 90 bp of 5' mltG
P1350	CATTATCCATTAAAATCAAACGGATCCTAAACTTCATC ATAGCCTTTACTTTCTAA		
Kan rpsL forward	TAGGATCCGTTGATTTTAATGGATAATG	$P_c-[kan-rpsL^+]$ cassette ^e	$P_c-[kan-rpsL^+]$
Kan rpsL reverse	GGGCCCTTCCTTATGCTTTG		
P1351	CAAAGCATAAGGAAAGGGGCCGATGTCACAGAAGG CAAGGTCTACTATG	D39	90 bp of 3' mltG and 3'

P1349	AGAGCAAACCTAGGAAACTAGCCGCAGGTTG		downstream fragment
For construction of K654 ($\Delta rodZ(spd_2050)::P_c-[kan-rpsL^+]$)			
TT329	CAACTGATATAGTTGGAAGTGAGGAGTCCATTCCC	D39	5' upstream fragment with 60 bp of 5' <i>rodZ</i>
P1386	CATTATCCATTAAAAATCAAACGGATCCTAATCAATCC CTGATTGATTCTAGCTAATCG		
Kan rpsL forward	TAGGATCCGTTGATTTTAATGGATAATG	$P_c-[kan-rpsL^+]$ cassette ^e	$P_c-[kan-rpsL^+$
Kan rpsL reverse	GGGCCCTTCCTTATGCTTTG		
P1387	CAAAGCATAAGGAAAGGGGCCGATTATCGAAATTA ACAGCTCAGACTGG	D39	60 bp of 3' <i>rodZ</i> and 3' downstream fragment
P1385	ACAACACCTGCAATGGCACACGTTGCTTT		

323

For transformation assays			
P1348	TCTTCTGCAGCCTTGAAAGAGGTGGCAGT	K637	$\Delta mltG::P_c\text{-}erm$
P1349	AGAGCAAACCTAGGAAACTAGCCGCAGGTTG		
TT452	GGAGGGTTGGCTGTGGGTGGCTACAAGAAC	IU7397	$\Delta pbp2b\text{<>}aad9$
TT352	TGAAGGACTGGAAAGACCCTGACCTTCT		
P1543	CAGGCCGTACTCTCTGTCCTCTTACTTCC	IU10943	$\Delta rodA::P_c\text{-}erm$
P1544	CGGGTGTCAAGCTCTGGCTTCATTTTC		
P1543	CAGGCCGTACTCTCTGTCCTCTTACTTCC	IU10945	$\Delta rodA::P_c\text{-}[kan-rpsL^+]$
P1544	CGGGTGTCAAGCTCTGGCTTCATTTTC		
AL35	GGGGGGCAAACCAAGTGATGTC	IU3897	$\Delta mreCD\text{<>}P_c\text{-}erm$
AL17	TGCTCCAACCTGAGGTGTTGAACC		
AL35	GGGGGGCAAACCAAGTGATGTC	IU1751	$\Delta mreCD\text{<>}aad9$
AL17	TGCTCCAACCTGAGGTGTTGAACC		
TT329	CAACTGATATAGTTGGAAGTGAGGAGTCCATTCCC	IU9931	$\Delta rodZ\text{<>}aad9$
P1385	ACAACACCTGCAATGGCACACGTTGCTTT		
TT329	CAACTGATATAGTTGGAAGTGAGGAGTCCATTCCC	E655	$\Delta rodZ::P_c\text{-}erm$
P1385	ACAACACCTGCAATGGCACACGTTGCTTT		
TT329	CAACTGATATAGTTGGAAGTGAGGAGTCCATTCCC	K654	$\Delta rodZ::P_c\text{-}[kan-rpsL^+]$
P1385	ACAACACCTGCAATGGCACACGTTGCTTT		
P222	CGTCGTGTGGCGCTGCTCAAATTGTT	E193	$\Delta pbp1b\text{::}P_c\text{-}erm$
P522	AACGGCAACCACCAAAGGAGAACCAAGGA		

324

Primers used for QRT-PCR		
		gene
AL031	CTGCGACAGCAGATTGACCACTA	spd_1874
AL032	TTCCTGAGGAGCTTCTCTGCAAC	
AL023	GGAGTAGCTGCCCTGTTGCAGTA	spd_0104
AL024	CAGGGCCATCGATAACCAACTCTT	
AL018	GTAGTGCTAAACAAATGGAGCCG	pcsB
AL019	GTCAATGCTTGAGCATCATCAGCC	
KK489	AAAGGTCGTGGTGGTAAGGGAATG	gyrA
KK490	GCATCTTGATCCAGGCGCATTACT	

325 ^aGenomic DNA of the indicated *S. pneumoniae* strains was used as templates for
 326 PCR reactions, except for P_c-erm and P_c-[kan-rpsL⁺] cassettes.

328 ^bGenotype of IU6929 is D39 Δcps pbp2x-HA-P_c-kan (Land *et al.*, 2013).

329 ^cGenotype of IU6565 is D39 Δcps ftsZ-FLAG-P_c-erm (Land *et al.*, 2013).

330 ^dGenotype of IU6962 is D39 Δcps ftsZ-Myc-P_c-kan (Land *et al.*, 2013).

331 ^eP_c-erm and P_c-kan-rpsL⁺ cassettes are described in (Tsui *et al.*, 2011).

332 ^fpJWV25 (Eberhardt *et al.*, 2009).

333 ^gStrain genotypes are listed in Supplemental Table S1.

334 ^hGenotype of IU8845 is D39 Δcps rpsL1 ftsZ-L₂-gfp (Winkler lab collection,
 335 unpublished), L₂-linker sequence is KLDIEFLQ (Fleurie *et al.*, 2014).

336 ⁱpKB01_mKate2 (Beilharz *et al.*, 2015).

337 ^jGenotype of IU9020 is D39 Δcps rpsL1 gfp-L₁-pbp2x (Winkler lab collection,
 338 unpublished). L₁ linker sequence is LEGSG The DNA template for gfp is pUC57-gfp(*Sp*)
 339 (Martin *et al.*, 2010).

340 ^kGenotype of IU3373 is D39 rpsL⁺-rpsG⁺-cat (Tsui *et al.*, 2010).

341 ^lIU8906 is an unpublised strain containing ΔbgaA::tet-P_{Zn} followed by 24 bp
 342 upstream of ftsA (RBS_{ftsA}). ΔbgaA::tet-P_{Zn} was obtained from pJWV25 (Eberhardt *et al.*,
 343 2009).

344 **Table S3.** Structural similarity of the extracellular domain of MltG_{Spn} to known protein
 345 structures

Aligned crystalized structure (organism, PDB ID) ^a	3D alignment coverage (MltG _{Spn} residues) ^{a,b}	Match confidence ^c (%)	RMSD (Å) ^d	Z-score ^e	2D domain ^f	Confirmed function
Lmo14992 (<i>L. monocytogenes</i> , 4I1W)	222-541	100	0.9	38.4	YceG-like (aa 87-248, cd08010)	no
MltG (<i>E. coli</i> , 2RIF)	266-547	100	3.7	31.4	YceG-like (aa 82-327, cd08010)	Lytic transglycosylase (Yunck <i>et al.</i> , 2015)
SleB (<i>B. anthracis</i> , 4FET)	411-533	97.1	1.5	7.6	Hydrolase_2 (aa 153-253, pfam07486)	Lytic transglycosylase (Heffron <i>et al.</i> , 2011)
SleB (<i>B. cereus</i> , 4F55)	412-460	94.7	3.6	8.1	Hydrolase_2 (aa 159-259, pfam07486)	no

346
 347 ^aResults were obtained from Phyre2 (Kelley & Sternberg, 2009) analysis by inputting
 348 amino acid sequence of the entire MltG_{Spn} and ran on intensive mode. Structures listed
 349 are >90% in match confidence.

350 ^bAmino acid residues of MltG_{Spn} aligned by Phyre2 analysis to protein structures in
 351 column 1. For Lmo14992, MltG_{Eco}, and SleB_{Ban}, the alignments cover the entire
 352 sequence of the crystalized peptide chains, which are aa 42-349, aa 81-340, and aa
 353 131-253, respectively, of these proteins. In contrast, only 49 residues of MltG_{Spn} align
 354 with aa 133-181 of the crystalized 123-residue SleB_{Bce} peptide.

355 ^cConfidence scores were obtained from Phyre2 analysis.

356 ^dRMSD values were determined via PyMOL alignment of the PDB modelling file
 357 generated from Phyre2 input of MltG sequence aligning with each homolog of *L.*

358 *monocytogenes*, *E.coli*, and *B. anthracis* using only the residues sequences shown in
359 column 2. Alignment of the *B. cereus* homolog was obtained with aa 411-533 of MltG_{Spn}
360 and aa 131-253 of the SleB_{Bce} peptide.

361 ^eZ-score was determined via input of the MltG PDB modeling file generated from
362 Phyre2 into the DALI server. Amino acid sequences used for the alignment and
363 generation of scores are the same as for RMSD.

364 ^fConserved domains identified by NCBI search

365 (<http://www.ncbi.nlm.nih.gov/Structure/cdd/wrpsb.cgi>) by inputting the complete amino
366 acid sequence of each protein listed in column 1. Domain names (YceG-like or
367 hydrolase_2) are followed in parenthesis by the residue numbers of each protein and
368 accession numbers of the domains. Residues 267 to 542 of MltG_{Spn} are identified as
369 YceG-like and cd08010).

370 **TABLE S4.** Genes encoding proteins with known or putative PG lytic domains and WalRK-regulated genes in *S.*
 371 *pneumoniae* serotype 2 strain D39^a, observed hydrolase activities in zymogram assays, and phenotypes of deletion
 372 mutants in a $\Delta pbp1a \Delta mltG$ background.

Gene or tag	Hydrolase class ^b	MW (kDa)	Missing band in zymogram ^c	Constructed deletion strain in IU7327 ($\Delta pbp1a \Delta mltG$) background ^e	Doubling time of triple deletion strain (min) ^f
<i>walK</i>	None, histidine kinase	51.7	ND ^d	IU7327	50.5 ± 5.5 (5)
<i>WalRK_{Spn}</i> regulon					
<i>pcsB</i>	Putative N-acetylmuramoyl-l-alanine amidase/endopeptidase	41.8	ND ^d	Essential in WT background ^g	
<i>lytB</i>	N-Acetylglucosaminidase	81.9	~80 kDa	IU9298	58.3 ± 15.5 (2)
<i>spd_1874</i>	Putative N-acetylmuramidase (LysM domain)	40.6	ND ^d	IU9292	55.3 (1)
<i>spd_0703</i>	None (putative SEDS protein)	11.0	ND ^d	IU9318	44 (1)
<i>spd_0104</i>	None (LysM domain)	17.8	ND ^d	IU9316	40.2 (1)
<i>spd_0126 (pspA)</i>	None	68.6	ND ^d	IU9320	51.1 ± 5.7 (2)
Cell division					
<i>pmp23</i>	Putative lytic transglycosylase	23.0	ND ^d	IU9290	62.9 ± 10.5 (3)
<i>dacA</i>	d,d-Carboxypeptidase	45.2	ND ^d	IU9386	ND ^h
<i>dacB (spd_0549)</i>	l,d-Carboxypeptidase	26.0	ND ^d	IU9388	ND ^h
Fraticide and autolysis during growth					
<i>lytA</i>	N-Acetylmuramoyl-l-alanine amidase	36.6	~36 kDa	IU9382	ND ^h
<i>cbpD</i>	Putative N-acetylmuramoyl-l-alanine amidase/endopeptidase	50.4	ND ^d	IU9384	40.4 (1)
<i>lytC</i>	N-Acetylmuramidase	57.4	~57 kDa	IU9294	53.1 ± 7.8 (2)

Other putative hydrolases that do not affect cell division					
spd_0873	Putative N-acetyl muramidase	30.1	ND ^d	IU9296	62.3 ± 12.6 (3)
spd_0173	Putative I,d-carboxypeptidase	38.8	ND ^d	IU9390	ND ^h

^aGrouping of genes based on (Barendt *et al.*, 2011).

^bBased on (Layec *et al.*, 2008).

^cZymogram assays were performed as described in *Supplemental experimental procedures*. Bands of indicated molecular weights were absent in the single $\Delta lytA$, $\Delta lytB$ or $\Delta lytC$ mutants when compared to the wild-type parent (See Fig. S8).

^dND, not determined

^eConstructed mutants with deleted gene in column 1 in IU7327 ($\Delta pbp1a \Delta mltG$) background. Strains IU10292 and IU10294 ($\Delta pbp1a \Delta mltG \Delta spd_0104$ and spd_1874) deleted for both LysM-domain proteins (Spd_0104 and Spd_1874) were also constructed. Only IU9235 ($\Delta pbp1a \Delta mltG \Delta walK$) among all the triple mutants showed significantly smaller colony size compared to the parent strain IU7327 after 24h incubation.

^fGrowth curves and doubling time determinations in BHI broth were performed as described in *Experimental procedures*. Most doubling times are the average and SEM of 2 to 5 independent growth experiments, indicated by n. Among the constructed triple mutants tested, only the triple $\Delta pbp1a \Delta mltG \Delta waIK$ mutant grew with a significantly longer doubling time than the $\Delta pbp1a \Delta mltG waIK^+$ parent.

388 ^g Since *pcsB* is essential for pneumococcal growth, it was not feasible to construct a $\Delta pbp1a \Delta mltG \Delta pcsB$ strain. We
389 investigated whether controlling expression of the essential *pcsB*⁺ gene from a promoter not regulated by the *WalRK* TCS
390 would improve the poor growth of the $\Delta pbp1a \Delta mltG \Delta walK$ mutant. We utilized the construct $\Delta bgaA'::kant1t2\text{-}P_{fcsK}\text{-}pcsB^+$,
391 which expresses *pcsB* from a fucose-controlled promoter (Barendt *et al.*, 2009) to a level similar to the expression from
392 the native *walK*-dependent promoter. We transformed a $\Delta walK$ amplicon into IU9330 ($\Delta pbp1a mltG(\Delta 488\text{bp}) P_{fcsK}\text{-}pcsB^+$)
393 in the presence or absence of 1 % fucose. We reasoned that if the poor growth of the $\Delta pbp1a mltG(\Delta 488\text{bp}) \Delta walK$ strain
394 was due solely to the under-expression of *pcsB*, the ectopic expression of *pcsB* from $P_{fcsK}\text{-}pcsB^+$ in the presence of fucose
395 would be able to overcome the growth defect. To the contrary, we observed that the transformants grew very poorly under
396 both inducing and non-inducing conditions. This result indicates that under-expression of *pcsB* alone does not account for
397 the poor growth of the $\Delta pbp1a \Delta mltG \Delta walK$ mutant.

398 ^hGrowth curves and of doubling time determinations in BHI broth were not determined; but colony sizes of the triple
399 mutants on TSAI-BA plates were similar to the control strain ($\Delta pbp1a \Delta mltG \Delta bgaA$).

400 **SUPPLEMENTAL FIGURE LEGENDS**

401 **Fig. S1.** Model of PG biosynthesis in ovococcus bacteria, such as *S. pneumoniae*,
402 and topology of proteins involved in peripheral PG synthesis. (A) Top. Ovococci divide
403 perpendicularly to their long axis (Zapun *et al.*, 2008). Unencapsulated derivatives of
404 serotype 2 strain D39 *S. pneumoniae* form mostly diplococci and chains of two cells,
405 whereas capsulated D39 strains form short chains of 8–10 cells (Barendt *et al.*, 2009).
406 Bottom. Formation of prolate-ellipsoid-shaped bacteria requires two modes of PG
407 synthesis, peripheral (sidewall-like) and septal PG synthesis, that occur in the midcell
408 region of dividing *S. pneumoniae* cells (Tsui *et al.*, 2014, Massidda *et al.*, 2013, Pinho *et*
409 *al.*, 2013, Sham *et al.*, 2012, Zapun *et al.*, 2008). At the start of a division cycle,
410 components of both peripheral PG synthesis complexes (orange ovals) and septal
411 synthesis complexes (green rectangles) locate to the equators of cells (bottom).
412 Peripheral PG synthesis (light blue; top) occurs between the future equator and septum
413 of dividing cells and may commence before septal synthesis (Massidda *et al.*, 2013,
414 Wheeler *et al.*, 2011, Zapun *et al.*, 2008). At some point, septal PG synthesis (medium
415 blue) commences to divide the cell in two. The complexes that carry out peripheral and
416 septal PG synthesis locate to a large constricting ring throughout the division cycle, with
417 the exception of PBP2x, which moves to the centers of septa in mid-to-late divisional
418 cells (Tsui *et al.*, 2014). The grey Pac-Man symbol corresponds to PG hydrolases that
419 remodel the PG and allow septal separation. Reproduced from (Tsui *et al.*, 2014). (B)
420 Topology of proteins (not drawn to scale) known or speculated to be involved in
421 peripheral PG synthesis in ovococci (Philippe *et al.*, 2014, Massidda *et al.*, 2013).
422 Involvement of MreC, MreD, PBP2b, and PBP1a in peripheral PG synthesis in

423 *Streptococcus pneumoniae* was shown experimentally in previous studies (Philippe et
424 al., 2014, Tsui et al., 2014, Berg et al., 2013, Massidda et al., 2014, Land & Winkler,
425 2011). This study shows that the MltG endo-LT is in the peripheral PG synthesis
426 machine, that MreCD and/or RodZ regulate PBP1a (arrows) and/or MltG activity and/or
427 localization, and that RodA controls activity of PBP2b (arrow), likely by direct interaction
428 (*Results and Discussion*). Figure is based on Philippe et al., 2014 and Massidda et al.,
429 2013 and work reported in this study.

430 **Fig. S2.** Phenotypes and Western blots of cells expressing epitope-tagged MltG
431 derivatives. Full genotypes of strains are listed in Table S1. Growth curves and Western
432 blotting were performed as described in *Experimental procedures and Supplemental*
433 *experimental procedures*. (A) and (B) Quantitative Western-blot analyses of strains
434 expressing MltG-FLAG (expected molecular mass = 62 kDa). Equal amounts (12 µg for
435 A, 26.5 µg for B) of total proteins from each strain with genotype indicated in the tables
436 were loaded onto each lane. Chemiluminescent signal intensity of each band was
437 normalized to the integrated intensity value obtained for IU9043 ($\Delta pbp1a\ mltG$ -FLAG) in
438 right panel of A, or B, or IU7403 ($mltG$ -FLAG, left panel of A). Relative signal intensities
439 (average \pm SEM) were obtained from two independent experiments. (C) Representative
440 growth curves of IU1945 parent, IU7399 ($mltG$ -HA) and IU7405 ($mltG$ -Myc). (D and E)
441 Western-blot analysis of untagged parent strain IU1945 (lane 1), and $mltG$ -HA (D,
442 IU7399, expected molecular mass = 62 kDa), and $mltG$ -Myc (E, IU7405, expected
443 molecular mass = 62 kDa).

444 **Fig. S3.** Domain architecture of YceG-domain proteins in bacteria of various cell
445 shapes. YceG-domain proteins of ovococci, including streptococci (*S. pneumoniae*, *S.*

446 *mitis*, *S. pyogenes*, *S. mutans*, and *S. agalactiae*) and *Lactococcus lactis*, have a similar
447 domain architecture consisting of an intracellular domain of 150 to 200 aa, a
448 transmembrane (TM) domain of ≈24 aa, and the extracellular YceG-like domain. The
449 intracellular domain of MltG_{Spn} (DUF_1346) has weak aa similarity to an intracellular
450 Mid-1 related chloride channel (MCLC) domain and to other DUFs (see *Results*). The
451 intracellular domain of *S. agalactiae* MltG has an DUF different from DUF_1346. The
452 intracellular domains of the MltG homologues of other ovoid species are predicted to be
453 disordered by Phyre2 analysis. Gram-positive rod-shaped bacteria, such as *Bacillus*
454 *subtilis* and *Listeria monocytogenes*, and Gram-negative rod-shaped bacterium *E. coli*
455 contain a short (<20 aa) intracellular domain. YceG domain proteins are absent in the
456 spherical bacterium *Staphylococcus aureus*. M designates membrane region. L
457 indicates a conserved LysM-like structure with a $\beta_1\alpha_1\alpha_2\beta_2\alpha_3$ fold that is a putative PG
458 binding domain. Strains and protein IDs used to generate this figure are: *S. pneumoniae*
459 D39 (ABJ53954.1), *S. mitis* B6 (YP_003446601), *S. pyogenes* A20 (YP_006932381.1),
460 *S. mutans* NN2025 (YP_003484312.1), *S. agalactiae* A909 (YP_330231), *Lactococcus*
461 *lactis* II1403 (NP_266791), *Bacillus subtilis* 168 (NP_390615), and *E. coli* K-12
462 (NP_415615.1).

463 **Fig. S4.** Scheme of experimental reconstruction of $\Delta pbp2b$ suppressor strains in
464 D39 Δcps *rpsL1* *pbp1a*⁺ background. See Supplemental *experimental procedures* for
465 details.

466 **Fig. S5.** Summary of stabilities and viabilities of strains containing frame-shift *mltG*
467 suppressor alleles. Strains containing frameshift *mltG* alleles (*sup2*, *sup4* and *sup5*) are
468 viable, but not stable in *pbp1a*⁺ or *pbp1a*⁺ $\Delta pbp2b$ genetic backgrounds. The following

469 Δ cps *pbp1a*⁺ strains showed non-uniform-sized colonies when streaked from ice stocks
470 onto TSAI BA plates: IU10342 (*pbp1a*⁺ *mltG*(E428Q)), the original suppressor strains
471 IU7477, IU7570, and IU7765, and reconstructed suppressor strains IU9777 (*pbp1a*⁺
472 *mltG*(Δ 5bp) Δ *pbp2b*), IU9905 (*pbp1a*⁺ *mltG*(Δ 488bp) Δ *pbp2b*) and IU9907 (*pbp1a*⁺
473 *mltG*(Ω 45bp)² Δ *pbp2b*). In contrast, strains containing Δ *mltG* or frameshift *mltG* alleles
474 are viable and stable in Δ *pbp1a* mutants (IU7325, IU7327, IU8549, IU8553 and
475 IU8555), or Δ *pbp1a* Δ *pbp2b* (IU7931, IU8565, IU8567, and IU8569) mutants (see Table
476 S1 for constructions and *Results* for additional details).

477 **Fig. S6.** Clustal Omega alignment of the transmembrane and extracellular domains
478 of MltG_{Eco}, MltG_{Spn}, and YceG_{Lmo} (the MltG homologue in *L. monocytogenes*). Letter
479 colors indicate the following aa properties: red: small, hydrophobic or aromatic; blue:
480 acidic; magenta: basic; green: hydroxyl, sulphydryl, or amine. The MltG_{Eco} sequence (gi:
481 accession 687676267) was aligned with MltG_{Spn} (gi: 116076234) and YceG_{Lmo} (gi:
482 16803539) using Clustal Omega (Sievers *et al.*, 2011) with default parameters. Symbols
483 indicate the following: asterisks (*) single fully conserved aa; colons (:), conservation
484 between groups with strongly similar properties; periods (.), conservation between
485 groups with weakly similar properties. The catalytic glutamate (E218 of MltG_{Eco} and
486 E428 of MltG_{Spn}) is indicated as E218/E428. Y488 of MltG_{Spn}, the aa changed in the
487 Δ *pbp2b sup3* strain, aligns with Y274 of MltG_{Eco} and is indicated as Y274/Y488.
488 Secondary structure information diagramed below the alignment was obtained from the
489 DSSP annotation in the sequence display feature of the PDB file (PDB ID: 4IIW). Start
490 and end sites mark the protein sequences used in the crystal structure determination of
491 YceG_{Lmo} (aa 26 to 349). See *Results*, *Discussion*, and Table S3 for additional details.

492 **Fig. S7.** (A) Superposition of crystalized region of YceG_{Lmo} (red, aa 42 to 349) and
493 MltG_{Spn} (blue, aa 266 to 547) backbones. Two distinct subdomains are in the YceG
494 domain: the N-terminal/membrane-proximal subdomain contains a LysM-like domain
495 with a $\beta_1\alpha_1\alpha_2\beta_2\alpha_3$ fold (inset) that is a putative PG binding site; and the C-terminal
496 catalytic subdomain with endo-LT activity. (B). Degree of conservation of each residue
497 in the LysM-like $\beta_1\alpha_1\alpha_2\beta_2\alpha_3$ subdomain (top line) and in the endo-LT catalytic subdomain
498 (bottom line), where asterisks mark the catalytic E aa and the Y aa changed in the sup3
499 allele. Color coded box at each residue was determined using the Consurf server
500 (Ashkenazy *et al.*, 2010) using amino acid sequences from MltG_{Lmo}. The residues within
501 $\beta_1\alpha_1\alpha_2\beta_2\alpha_3$ folds are mostly conserved. The catalytic E and Y residues are highly
502 conserved. See *Results*, *Discussion*, and Table S3 for additional details.

503 **Fig. S8.** Zymogram of membrane extracts from strain IU1945 (wild-type
504 unencapsulated parent) and isogenic PG hydrolase mutants K43 ($\Delta lytA$), K27 ($\Delta lytB$),
505 and K5 ($\Delta lytC$). Electrophoresis of membrane extracts was performed in an SDS-12%
506 polyacrylamide gel containing a lysed-cell preparation of IU1945 (D39 Δcps) as PG
507 substrate. Membrane extracts from the strains and lysed-cell PG substrate were
508 prepared and subjected to zymography as described in *Supplemental experimental*
509 *procedures*. Equal amounts of proteins (35 μ g) were loaded into each lane. Lane
510 molecular weight (MW) markers (PageRuler prestained protein ladder, Thermo
511 Scientific) calibrated by the vendor are shown at left. Arrows to the right of the gel
512 indicate the migration positions of LytA, LytB, and LytC as inferred by absence of bands
513 in the corresponding deletion mutants. MltG endo-LT activity is expected to overlap the
514 upper intact LytC band and would be visible in the $\Delta lytC$ lane.

515 **Fig. S9.** Growth phenotypes and cell morphologies of *mltG*(ΔDUF_1346) mutant
516 strain IU9025 compared to that of its *mltG*⁺ parent strain IU1824. Experiments were
517 carried out as described in *Supplemental experimental procedures*. (A) Slight growth
518 defect of IU9025 (*mltG*(ΔDUF_1346)) compared to IU1824 (*mltG*⁺ parent) under high
519 salt conditions. (B) Marginal difference in sensitivity of IU9025 (*mltG*(ΔDUF_1346)) to
520 penicillin G compared to IU1824 (*mltG*⁺ parent). (C) No difference in growth of IU1824
521 (*mltG*⁺) and IU9025 (*mltG*(ΔDUF_1346)) in BHI broth at neutral or low pH conditions.
522 (D) IU9025 (*mltG*(ΔDUF_1346)) and IU1824 (*mltG*⁺) cells have the same length and
523 width within experimental error.

524 **Fig. S10.** Growth curves of *mltG*⁺ parent strain IU1945 (D39 Δcps) and merodiploid
525 strain IU9102 ($\Delta mltG/\Delta bgaA::P_{Zn}-mltG$) in the absence or presence of different
526 concentrations of the inducer Zn²⁺. IU1945 and IU9102 were grown overnight in BHI
527 broth containing 0.2 mM ZnCl₂ and 0.02 mM MnSO₄, centrifuged to remove Zn²⁺ and
528 Mn²⁺, and resuspended to OD₆₂₀ ≈ 0.005 in BHI broth containing 0.2 mM ZnCl₂ and 0.02
529 mM MnSO₄, 0.1 mM ZnCl₂ and 0.01 mM MnSO₄, or 0.05 mM ZnCl₂ and 0.005 mM
530 MnSO₄, or no Zn²⁺ and Mn²⁺ (0 mM Zn) as described in *Experimental procedures*. Tenth
531 the concentration of MnSO₄ was added to prevent effects of zinc toxicity (Jacobsen *et*
532 *al.*, 2011).

533 **Fig. S11.** Representative growth curves and morphological changes of $\Delta pbp1a$,
534 $\Delta pbp1a \Delta mltG$ and $\Delta pbp1a \Delta mltG \Delta pbp2b$ strains. Strains IU1824 (1, D39 Δcps parent),
535 IU6741 (2, $\Delta pbp1a$), IU7327 (3, $\Delta pbp1a \Delta mltG$) and IU7931 (4, $\Delta pbp1a \Delta mltG \Delta pbp2b$)
536 were grown overnight in BHI and diluted to OD₆₂₀ ≈ 0.003 in BHI to start growth cultures
537 as described in *Experimental procedures*. (A) Representative growth curves. Doubling

times (mean \pm SEM) for IU1824, IU6741, IU7327 and IU7931 were 38 ± 1 (n=4), 48 ± 3 (n=3), 46 ± 4 (n=2), and 48 ± 3 (n=2) respectively, and were not statistically different from each other by one-way ANOVA analysis (GraphPad Prism, nonparametric Kruskal-Wallis test)). (B) Phase-contrast images of strains growing in exponential phase ($OD_{620} \approx 0.15$). Micrographs are at the same magnification (scale bars = 1 μ m). (C) Box-and-whisker plots (whiskers, 5 and 95 percentile) of cell lengths, widths, aspect ratios (length to width ratio) and relative volumes. Fifty or more cells from two independent experiments were measured as described in *Experimental procedures* for each strain. P values were obtained by one-way ANOVA analysis (GraphPad Prism, nonparametric Kruskal-Wallis test). *** denotes p<0.001.

Fig. S12. (A) Appearance of colonies on TSAI-BA plates of strains IU1690 (D39 *cps*⁺), IU9771 (*cps*⁺ $\Delta mltG$), IU9897 (*cps*⁺ $\Delta mltG \Delta pbp2b$), and IU10021 (*cps*⁺ $\Delta mltG \Delta pbp1a$). Frozen stocks of strains were streaked onto TSAI-BA plates and photographed after 17 h of incubation at 37°C. (B) Transformation of a $\Delta cps2E$ amplicon into IU9771 (D39 *cps*⁺ $\Delta mltG$) to obtain an unencapsulated strain results in accumulations of spontaneous mutations in *pbp1a*. Two isolates (IU9899 and IU10048) obtained from two independent transformations were sequenced for the *pbp1a* region. IU9899 contained *pbp1a*($\Delta T@F33$) and IU10048 contained *pbp1a*(G559stop (GGA→TGA)) mutations.

Fig. S13. Larger width of MltG-HA rings compared to FL-V rings detected by 2D and 3D-SIM IFM. Strain IU7399 (*mltG*-HA) was grown in BHI broth and processed for FL-V staining, IFM, and DAPI labeling as described in *Experimental procedures*. (A) Representative images of a field of cells stained with FL-V and subjected to 2D IFM to

561 detect MltG-HA localization. (B) Representative 3D-SIM IFM and FL-V images of cells
562 at division stages 1-4, (C) averaged 2D IFM images and fluorescence intensity traces,
563 and (D) scatter plots of FL-V labeling width versus MltG width at midcell equators and
564 septa at division stages 1-4 in (C) were obtained and processed as described for Fig.
565 10, except FL-V images are colored green. In D, *** denotes $p<0.001$. Representative
566 images in (A) and (B), and data in (C) and (D) were obtained from two independent
567 biological replicates.

568 **Fig. S14.** Representative growth curves and doubling times of mutants containing
569 $\Delta walK$ or single deletion mutations in known and putative PG hydrolase genes in (A)
570 wild-type *pbp1a⁺* strain IU1824, and in (B) $\Delta pbp1a \Delta mltG$ mutant strain IU7327 (see
571 Table S1). Doubling times are the averages \pm SEM from 2 to 5 independent growths for
572 most strains or from one growth ($n=1$) in some cases.

573 **Fig. S15.** Induction of WalRK regulon members in strains containing *mltG*(Δ 488bp)
574 or *mltG*(Y488D) mutations. RNA preparation and QRT-PCR procedures to determine
575 relative transcript amounts of *spd_1874*, *spd_0104*, and *pcsB* were performed as
576 described in *Supplemental experimental procedures* for isogenic strains IU1824 (D39
577 $\Delta cps rpsL1$, wild-type (WT) parent), IU6741 ($\Delta pbp1a$), IU8553 ($\Delta pbp1a mltG(\Delta 488bp)$),
578 IU8567 ($\Delta pbp1a mltG(\Delta 488bp) \Delta pbp2b$), IU9760 (*mltG*(Y488D)), and IU9783
579 (*mltG*(Y488D) $\Delta pbp2b$). Numbers at top of each bar indicate the average fold changes
580 of transcript amounts relative to the WT parent based on three independent QRT-PCR
581 experiments from three independent biological replicates. *, **, *** indicate p values
582 <0.05, <0.01 and <0.001, respectively using a one-sample t test to determine if the

583 mean was significantly different from a hypothetical value of 1. See *Results* and
584 *Discussion* for additional details.

585

586 REFERENCES TO SUPPLEMENTAL INFORMATION

- 587 Ashkenazy, H., E. Erez, E. Martz, T. Pupko & N. Ben-Tal, (2010) ConSurf 2010:
588 calculating evolutionary conservation in sequence and structure of proteins and
589 nucleic acids. *Nuc Acids Res* **38**: W529-533.
- 590 Barendt, S.M., A.D. Land, L.T. Sham, W.L. Ng, H.C. Tsui, R.J. Arnold & M.E. Winkler,
591 (2009) Influences of capsule on cell shape and chain formation of wild-type and
592 *pcnB* mutants of serotype 2 *Streptococcus pneumoniae*. *J Bacteriol* **191**: 3024-
593 3040.
- 594 Barendt, S.M., L.T. Sham & M.E. Winkler, (2011) Characterization of mutants deficient
595 in the L,D-carboxypeptidase (DacB) and WalRK (VicRK) regulon, involved in
596 peptidoglycan maturation of *Streptococcus pneumoniae* serotype 2 strain D39. *J*
597 *Bacteriol* **193**: 2290-2300.
- 598 Bartual, S.G., D. Straume, G.A. Stamsas, I.G. Munoz, C. Alfonso, M. Martinez-Ripoll,
599 L.S. Havarstein & J.A. Hermoso, (2014) Structural basis of PcsB-mediated cell
600 separation in *Streptococcus pneumoniae*. *Nature Comm* **5**: 3842.
- 601 Beilharz, K., R. van Raaphorst, M. Kjos & J.W. Veening, (2015) Red fluorescent
602 proteins for gene expression and protein localization studies in *Streptococcus*
603 *pneumoniae* and efficient transformation with Gibson assembled DNA. *App*
604 *Environl Microbiol*.
- 605 Benjamini, Y. & Y. Hochberg, (1995) Controlling the False Discovery Rate - a Practical
606 and Powerful Approach to Multiple Testing. *J Roy Stat Soc B Met* **57**: 289-300.
- 607 Berg, K.H., G.A. Stamsas, D. Straume & L.S. Havarstein, (2013) Effects of low PBP2b
608 levels on cell morphology and peptidoglycan composition in *Streptococcus*
609 *pneumoniae* R6. *J Bacteriol* **195**: 4342-4354.
- 610 Eberhardt, A., L.J. Wu, J. Errington, W. Vollmer & J.W. Veening, (2009) Cellular
611 localization of choline-utilization proteins in *Streptococcus pneumoniae* using
612 novel fluorescent reporter systems. *Molec Microbiol* **74**: 395-408.
- 613 Evan, G.I., G.K. Lewis, G. Ramsay & J.M. Bishop, (1985) Isolation of monoclonal
614 antibodies specific for human c-myc proto-oncogene product. *Mol Cell Biol* **5**:
615 3610-3616.
- 616 Fleurie, A., S. Manuse, C. Zhao, N. Campo, C. Cluzel, J.P. Lavergne, C. Freton, C.
617 Combet, S. Guiral, B. Soufi, B. Macek, E. Kuru, M.S. VanNieuwenhze, Y.V. Brun,
618 A.M. Di Guilmi, J.P. Claverys, A. Galinier & C. Grangeasse, (2014) Interplay of
619 the serine/threonine-kinase StkP and the paralogs DivIVA and GpsB in
620 pneumococcal cell elongation and division. *PLoS Genet* **10**: e1004275.
- 621 Heffron, J.D., N. Sherry & D.L. Popham, (2011) In vitro studies of peptidoglycan binding
622 and hydrolysis by the *Bacillus anthracis* germination-specific lytic enzyme SleB. *J*
623 *Bacteriol* **193**: 125-131.

- 624 Hopp, T.P., K.S. Prickett, V.L. Price, R.T. Libby, C.J. March, D.P. Cerretti, D.L. Urdal &
625 P.J. Conlon, (1988) A short polypeptide marker sequence useful for recombinant
626 protein identification and purification. *BioTechnol* **6**: 1204-1210.
- 627 Jacobsen, F.E., K.M. Kazmierczak, J.P. Lisher, M.E. Winkler & D.P. Giedroc, (2011)
628 Interplay between manganese and zinc homeostasis in the human pathogen
629 *Streptococcus pneumoniae*. *Metallomics* **3**: 38-41.
- 630 Kelley, L.A. & M.J. Sternberg, (2009) Protein structure prediction on the Web: a case
631 study using the Phyre server. *Nature Protos* **4**: 363-371.
- 632 Kocaoglu, O., H.C. Tsui, M.E. Winkler & E.E. Carlson, (2015) Profiling of beta-Lactam
633 Selectivity for Penicillin-Binding Proteins in *Streptococcus pneumoniae* D39.
634 *Antimicrob Agents Chemother* **59**: 3548-3555.
- 635 Land, A.D., H.C. Tsui, O. Kocaoglu, S.A. Vella, S.L. Shaw, S.K. Keen, L.T. Sham, E.E.
636 Carlson & M.E. Winkler, (2013) Requirement of essential Pbp2x and GpsB for
637 septal ring closure in *Streptococcus pneumoniae* D39. *Molec Microbiol* **90**: 939-
638 955.
- 639 Land, A.D. & M.E. Winkler, (2011) The requirement for pneumococcal MreC and MreD
640 is relieved by inactivation of the gene encoding PBP1a. *J Bacteriol* **193**: 4166-
641 4179.
- 642 Langmead, B. & S.L. Salzberg, (2012) Fast gapped-read alignment with Bowtie 2.
643 *Nature Methods* **9**: 357-359.
- 644 Langmead, B., C. Trapnell, M. Pop & S.L. Salzberg, (2009) Ultrafast and memory-
645 efficient alignment of short DNA sequences to the human genome. *Genome Biol*
646 **10**: R25.
- 647 Lanie, J.A., W.L. Ng, K.M. Kazmierczak, T.M. Andrzejewski, T.M. Davidsen, K.J.
648 Wayne, H. Tettelin, J.I. Glass & M.E. Winkler, (2007) Genome sequence of
649 Avery's virulent serotype 2 strain D39 of *Streptococcus pneumoniae* and
650 comparison with that of unencapsulated laboratory strain R6. *J Bacteriol* **189**: 38-
651 51.
- 652 Layec, S., B. Decaris & N. Leblond-Bourget, (2008) Diversity of Firmicutes
653 peptidoglycan hydrolases and specificities of those involved in daughter cell
654 separation. *Res Microbiol* **159**: 507-515.
- 655 Li, H., B. Handsaker, A. Wysoker, T. Fennell, J. Ruan, N. Homer, G. Marth, G.
656 Abecasis, R. Durbin & S. Genome Project Data Processing, (2009) The
657 sequence alignment/map format and SAMtools. *Bioinform* **25**: 2078-2079.
- 658 Lohse, M., A.M. Bolger, A. Nagel, A.R. Fernie, J.E. Lunn, M. Stitt & B. Usadel, (2012)
659 RobiNA: a user-friendly, integrated software solution for RNA-Seq-based
660 transcriptomics. *Nuc Acids Res* **40**: W622-627.
- 661 Love, M.I., W. Huber & S. Anders, (2014) Moderated estimation of fold change and
662 dispersion for RNA-seq data with DESeq2. *Genome biology* **15**.
- 663 Margulies, M., M. Egholm, W.E. Altman, S. Attiya, J.S. Bader, L.A. Bemben, J. Berka,
664 M.S. Braverman, Y.J. Chen, Z. Chen, S.B. Dewell, L. Du, J.M. Fierro, X.V.
665 Gomes, B.C. Godwin, W. He, S. Helgesen, C.H. Ho, G.P. Irzyk, S.C. Jando, M.L.
666 Alenquer, T.P. Jarvie, K.B. Jirage, J.B. Kim, J.R. Knight, J.R. Lanza, J.H.
667 Leamon, S.M. Lefkowitz, M. Lei, J. Li, K.L. Lohman, H. Lu, V.B. Makijani, K.E.
668 McDade, M.P. McKenna, E.W. Myers, E. Nickerson, J.R. Nobile, R. Plant, B.P.

- 669 Puc, M.T. Ronan, G.T. Roth, G.J. Sarkis, J.F. Simons, J.W. Simpson, M.
670 Srinivasan, K.R. Tartaro, A. Tomasz, K.A. Vogt, G.A. Volkmer, S.H. Wang, Y.
671 Wang, M.P. Weiner, P. Yu, R.F. Begley & J.M. Rothberg, (2005) Genome
672 sequencing in microfabricated high-density picolitre reactors. *Nature* **437**: 376-
673 380.
- 674 Martin, B., C. Granadel, N. Campo, V. Henard, M. Prudhomme & J.P. Claverys, (2010)
675 Expression and maintenance of ComD-ComE, the two-component signal-
676 transduction system that controls competence of *Streptococcus pneumoniae*.
677 *Molc Microbiol* **75**: 1513-1528.
- 678 Massidda, O., L. Novakova & W. Vollmer, (2013) From models to pathogens: how much
679 have we learned about *Streptococcus pneumoniae* cell division? *Environ*
680 *Microbiol*.
- 681 Philippe, J., T. Vernet & A. Zapun, (2014) The elongation of ovococci. *Microb Drug*
682 *Resist* **20**: 215-221.
- 683 Pinho, M.G., M. Kjos & J.W. Veening, (2013) How to get (a)round: mechanisms
684 controlling growth and division of coccoid bacteria. *Nat Rev Microbiol* **11**: 601-
685 614.
- 686 Ramos-Montanez, S., K.M. Kazmierczak, K.L. Hentchel & M.E. Winkler, (2010)
687 Instability of ackA (acetate kinase) mutations and their effects on acetyl
688 phosphate and ATP amounts in *Streptococcus pneumoniae* D39. *J Bacteriol* **192**:
689 6390-6400.
- 690 Robinson, M.D., D.J. McCarthy & G.K. Smyth, (2010) edgeR: a Bioconductor package
691 for differential expression analysis of digital gene expression data. *Bioinform* **26**:
692 139-140.
- 693 Sham, L.T., H.C. Tsui, A.D. Land, S.M. Barendt & M.E. Winkler, (2012) Recent
694 advances in pneumococcal peptidoglycan biosynthesis suggest new vaccine and
695 antimicrobial targets. *Curr Opinion Microbiol* **15**: 194-203.
- 696 Sievers, F., A. Wilm, D. Dineen, T.J. Gibson, K. Karplus, W. Li, R. Lopez, H. McWilliam,
697 M. Remmert, J. Soding, J.D. Thompson & D.G. Higgins, (2011) Fast, scalable
698 generation of high-quality protein multiple sequence alignments using Clustal
699 Omega. *Molec Sys Biol* **7**: 539.
- 700 Thibessard, A., A. Fernandez, B. Gintz, N. Leblond-Bourget & B. Decaris, (2002) Effects
701 of rodA and pbp2b disruption on cell morphology and oxidative stress response
702 of *Streptococcus thermophilus* CNRZ368. *J Bacteriol* **184**: 2821-2826.
- 703 Tsui, H.C., D. Mukherjee, V.A. Ray, L.T. Sham, A.L. Feig & M.E. Winkler, (2010)
704 Identification and characterization of noncoding small RNAs in *Streptococcus*
705 *pneumoniae* serotype 2 strain D39. *J Bacteriol* **192**: 264-279.
- 706 Tsui, H.C., S.K. Keen, L.T. Sham, K.J. Wayne & M.E. Winkler, (2011) Dynamic
707 distribution of the SecA and SecY translocase subunits and septal localization of
708 the HtrA surface chaperone/protease during *Streptococcus pneumoniae* D39 cell
709 division. *mBio* **2**: e00202-11.
- 710 Tsui, H.C., M.J. Boersma, S.A. Vella, O. Kocaoglu, E. Kuru, J.K. Peceny, E.E. Carlson,
711 M.S. VanNieuwenhze, Y.V. Brun, S.L. Shaw & M.E. Winkler, (2014) Pbp2x
712 localizes separately from Pbp2b and other peptidoglycan synthesis proteins

- 713 during later stages of cell division of *Streptococcus pneumoniae* D39. *Molec*
714 *Microbiol* **94**: 21-40.
- 715 Wayne, K.J., L.T. Sham, H.C. Tsui, A.D. Gutu, S.M. Barendt, S.K. Keen & M.E. Winkler,
716 (2010) Localization and cellular amounts of the WalRKJ (VicRKX) two-
717 component regulatory system proteins in serotype 2 *Streptococcus pneumoniae*.
718 *J Bacteriol* **192**: 4388-4394.
- 719 Wheeler, R., S. Mesnage, I.G. Boneca, J.K. Hobbs & S.J. Foster, (2011) Super-
720 resolution microscopy reveals cell wall dynamics and peptidoglycan architecture
721 in ovococcal bacteria. *Molec Microbiol* **82**: 1096-1109.
- 722 Wilson, I.A., H.L. Niman, R.A. Houghten, A.R. Cherenson, M.L. Connolly & R.A. Lerner,
723 (1984) The structure of an antigenic determinant in a protein. *Cell* **37**: 767-778.
- 724 Yunck, R., H. Cho & T.G. Bernhardt, (2015) Identification of MltG as a potential
725 terminase for peptidoglycan polymerization in bacteria. *Molec Microbio* doi:
726 10.1111/mmi.13258.
- 727 Zapun, A., T. Vernet & M.G. Pinho, (2008) The different shapes of cocci. *FEMS Microb*
728 *Rev* **32**: 345-360.

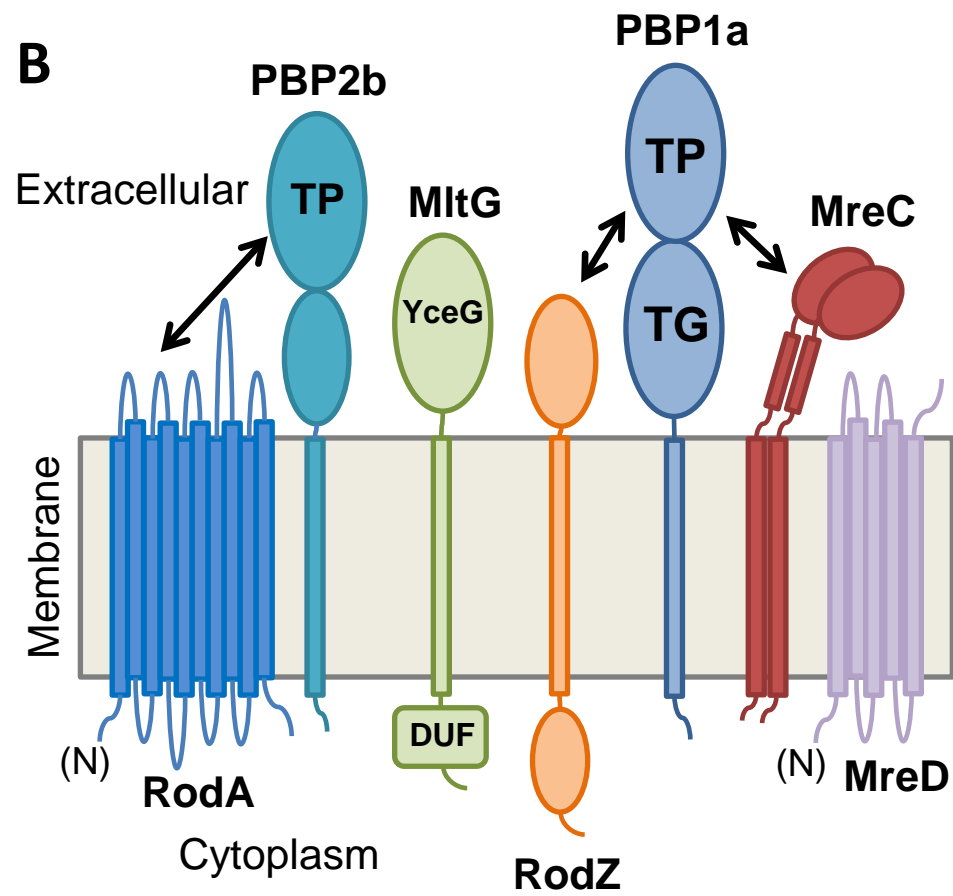
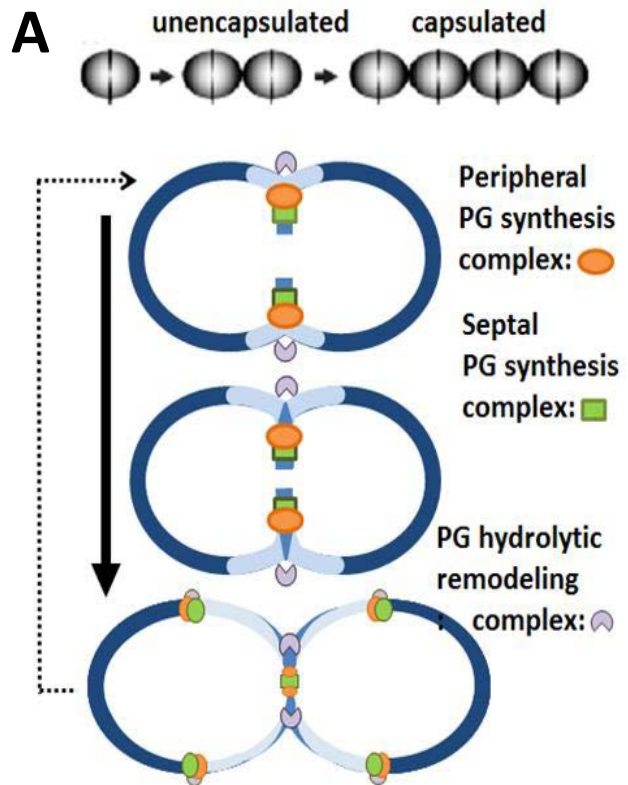


Fig. S1

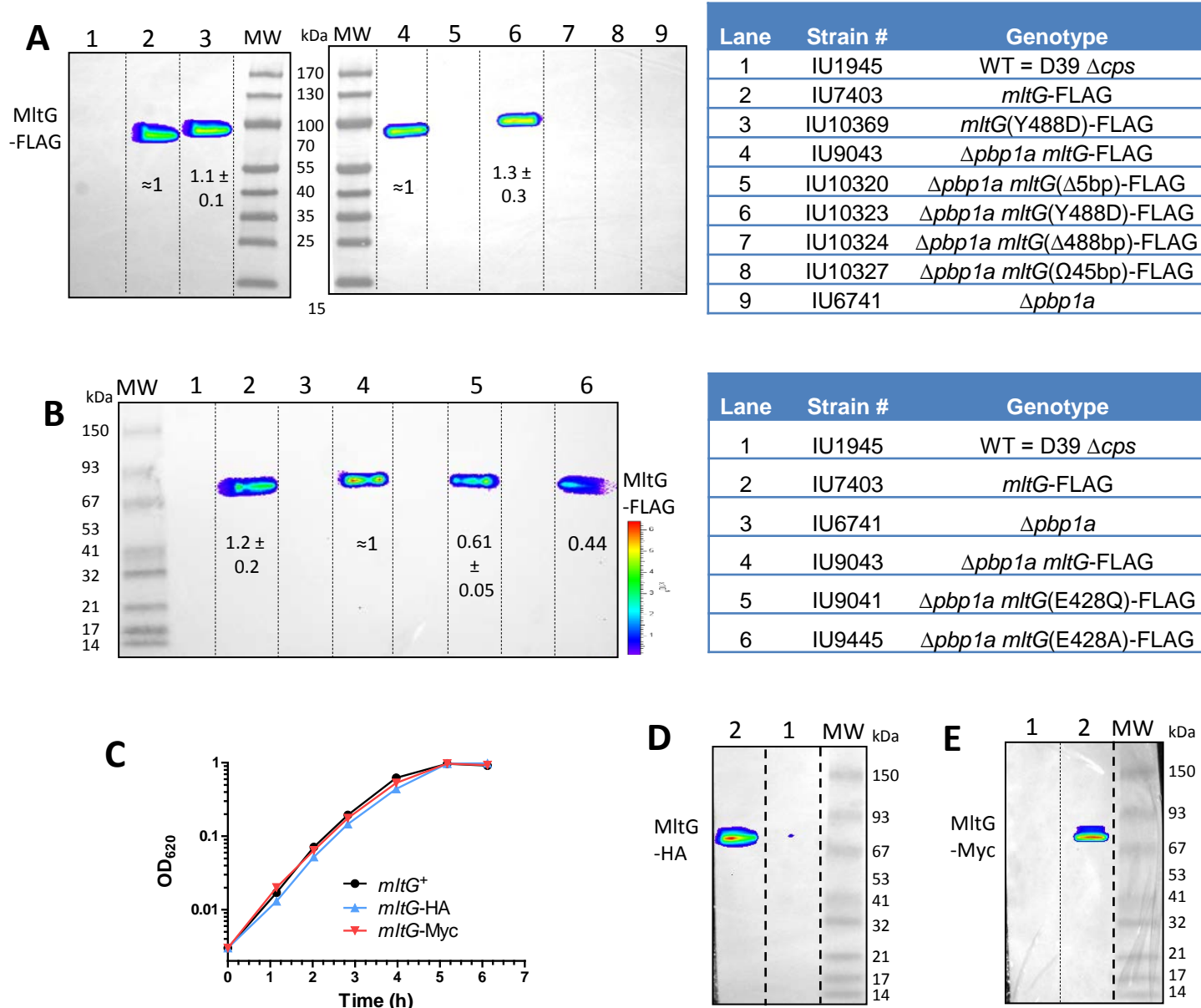


Fig. S2

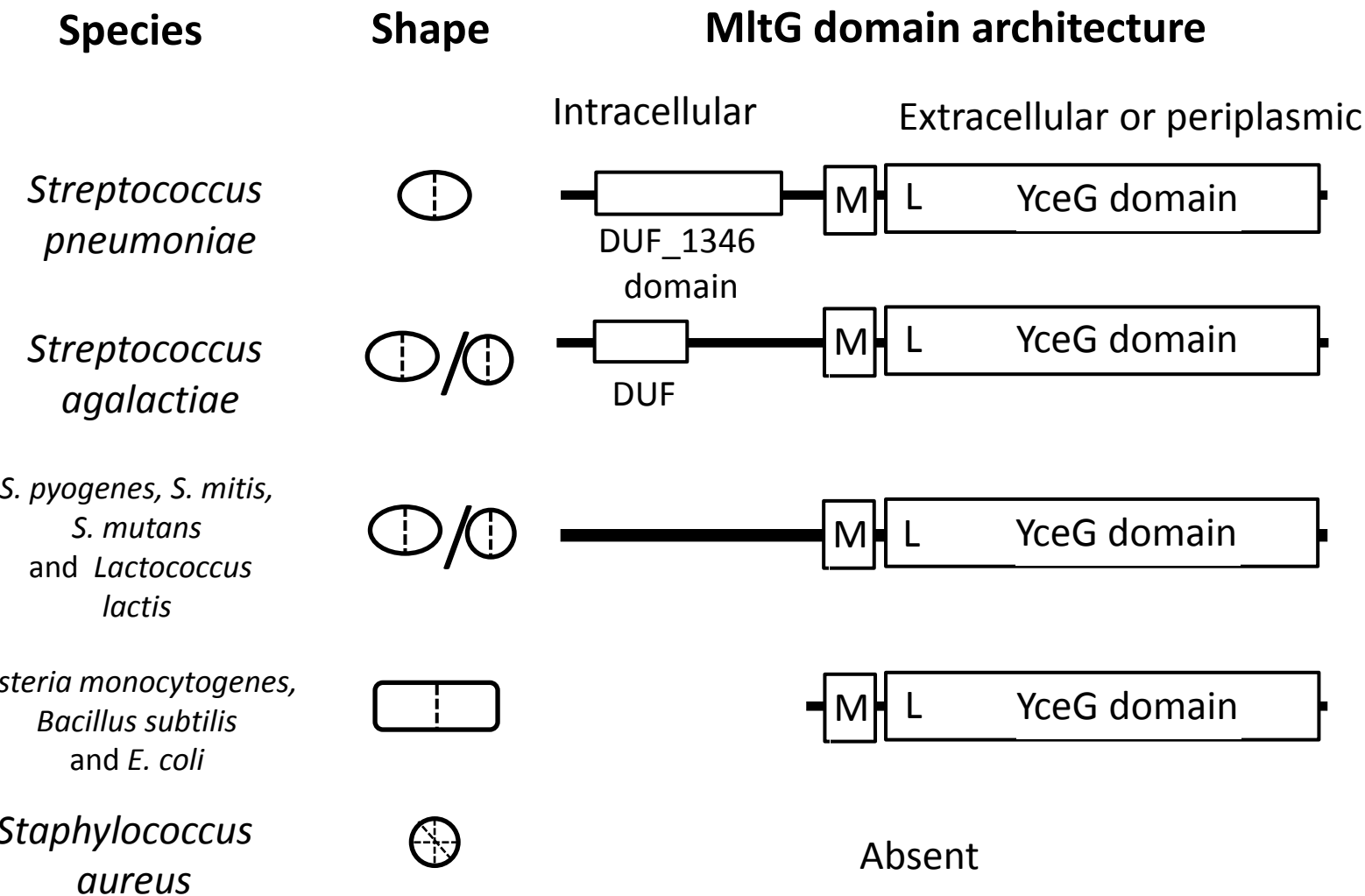


Fig. S3

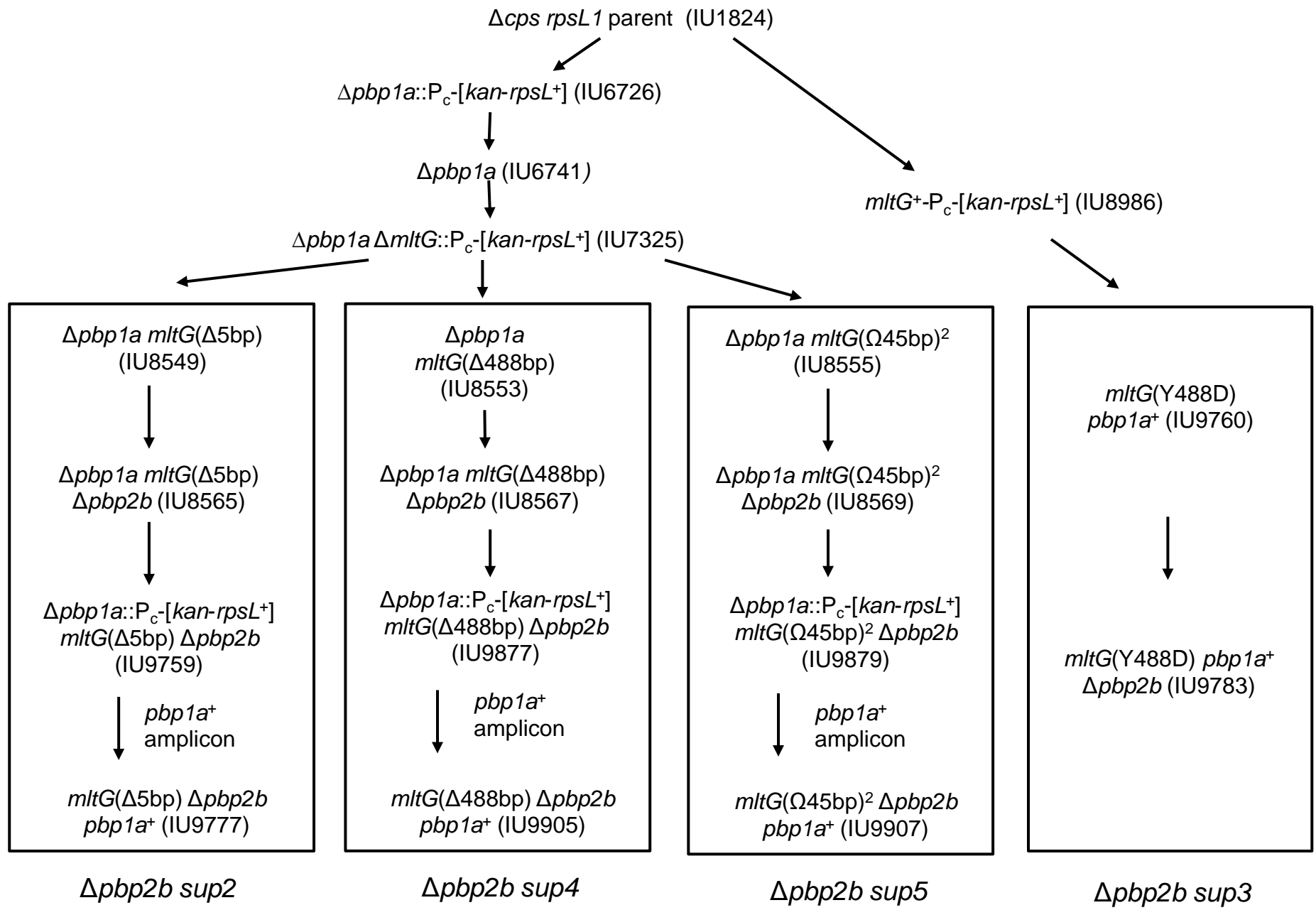


Fig. S4

Viable, but not stable (picks up suppressors):

$mltG(E428Q)$ $pbp1a^+$

[$mltG(\Delta 5\text{bp})$, $mltG(\Delta 488\text{bp})$, or $mltG(\Omega 45\text{bp})^2$] $\Delta pbp2b$

Viable and stable:

$\Delta mltG$ $\Delta pbp1a$

[$mltG(\Delta 5\text{bp})$, $mltG(\Delta 488\text{bp})$, or $mltG(\Omega 45\text{bp})^2$] $\Delta pbp1a$

$\Delta mltG$ $\Delta pbp1a$ $\Delta pbp2b$

$mltG(\Delta 5\text{bp})$ $\Delta pbp1a$ $\Delta pbp2b$

$mltG(\Delta 488\text{bp})$ $\Delta pbp1a$ $\Delta pbp2b$

$mltG(\Omega 45\text{bp})^2$ $\Delta pbp1a$ $\Delta pbp2b$

$sup2 = mltG(\Delta 5\text{bp})$

$sup4 = mltG(\Delta 488\text{bp})$

$sup5 = mltG(\Omega 45\text{bp})^2$

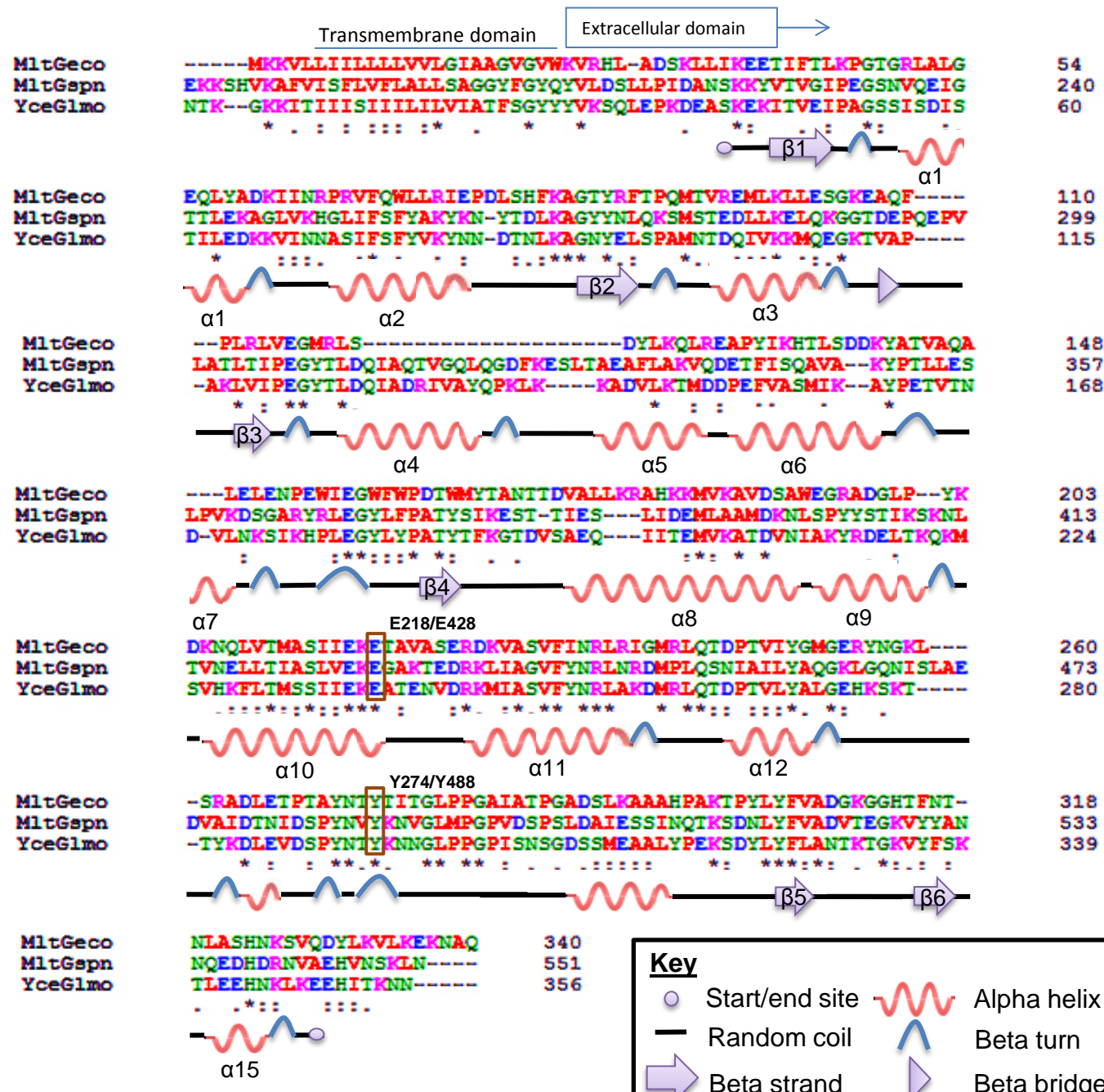


Fig. S6

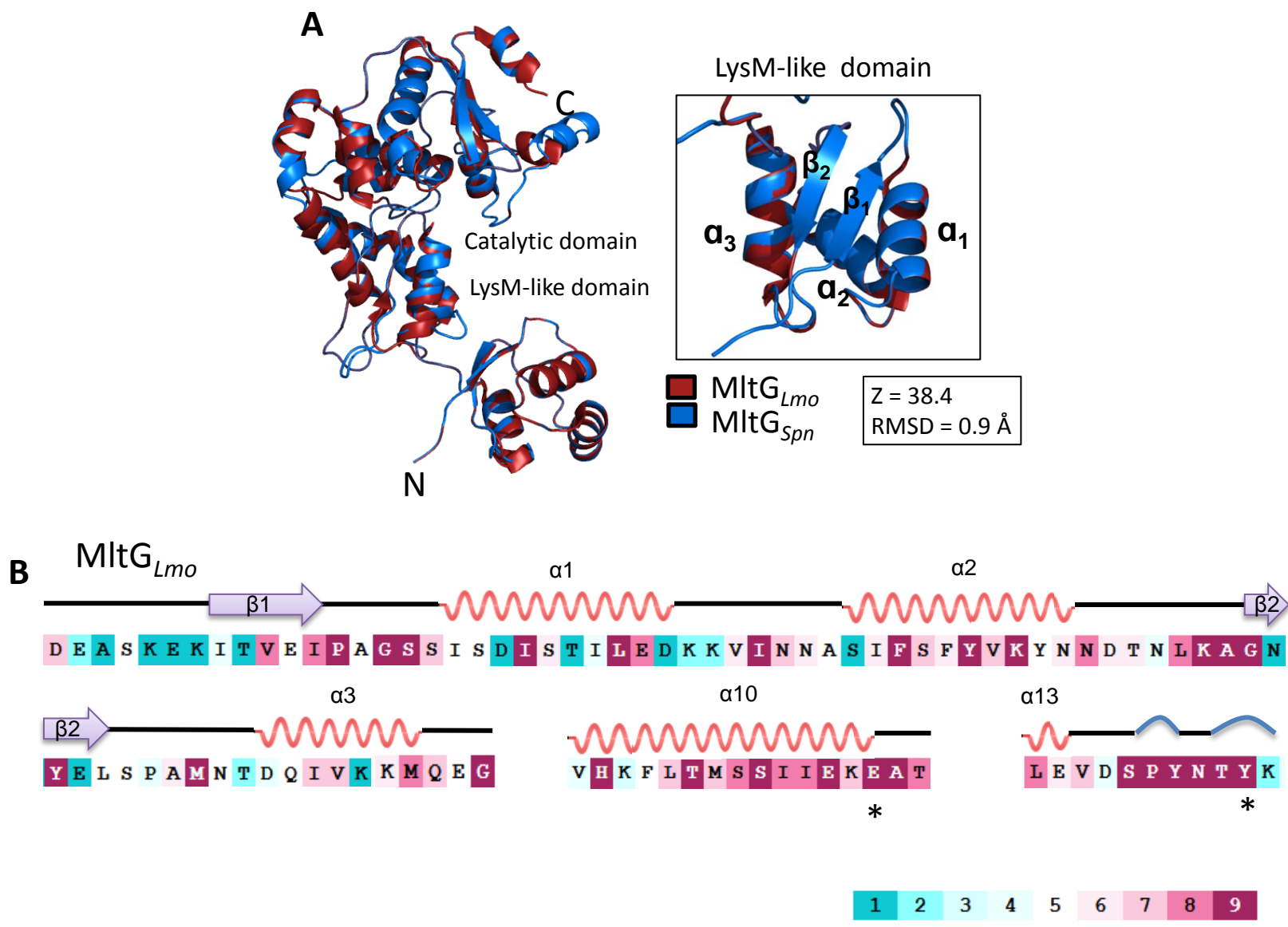


Fig. S7

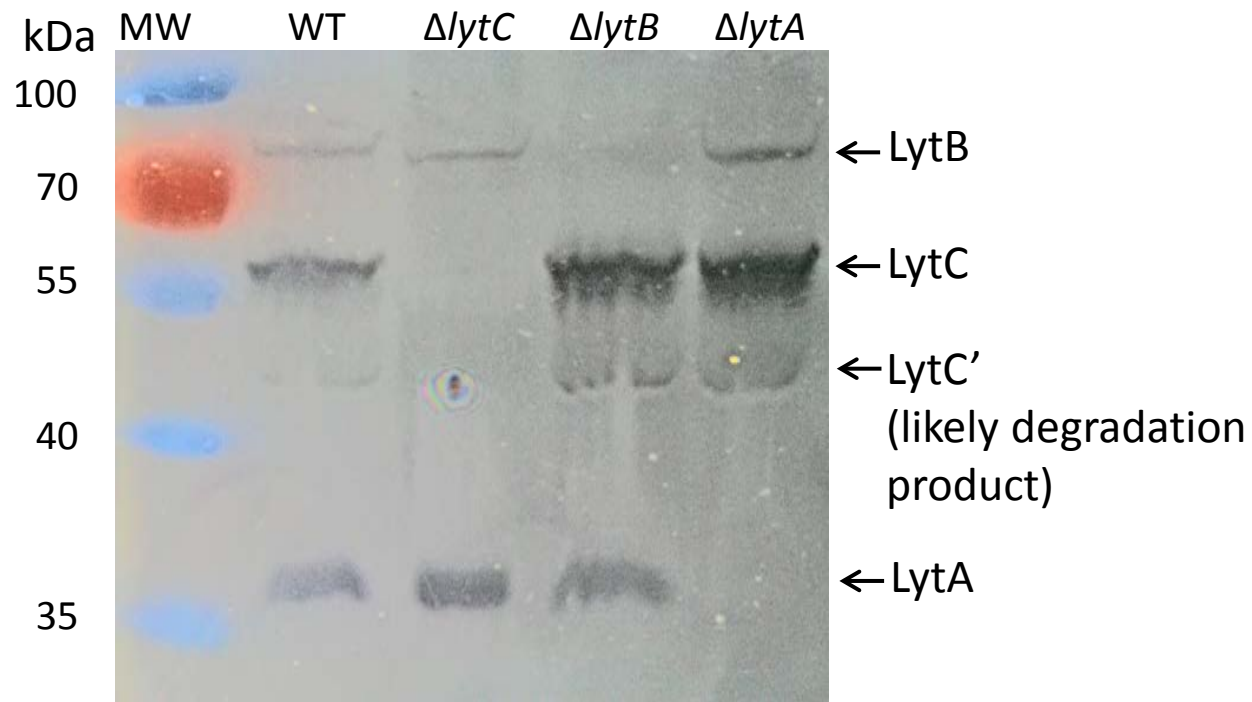


Fig. S8

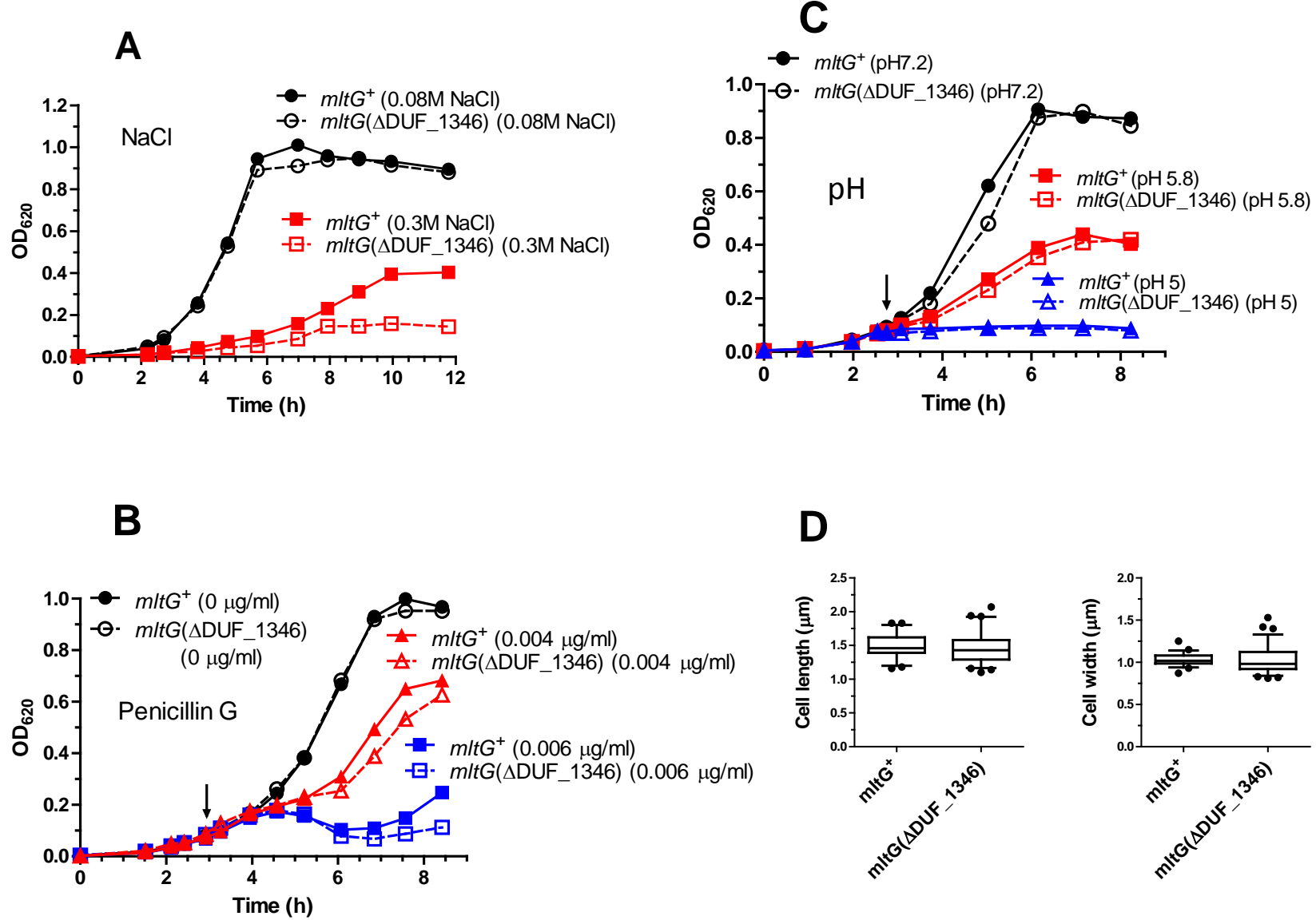
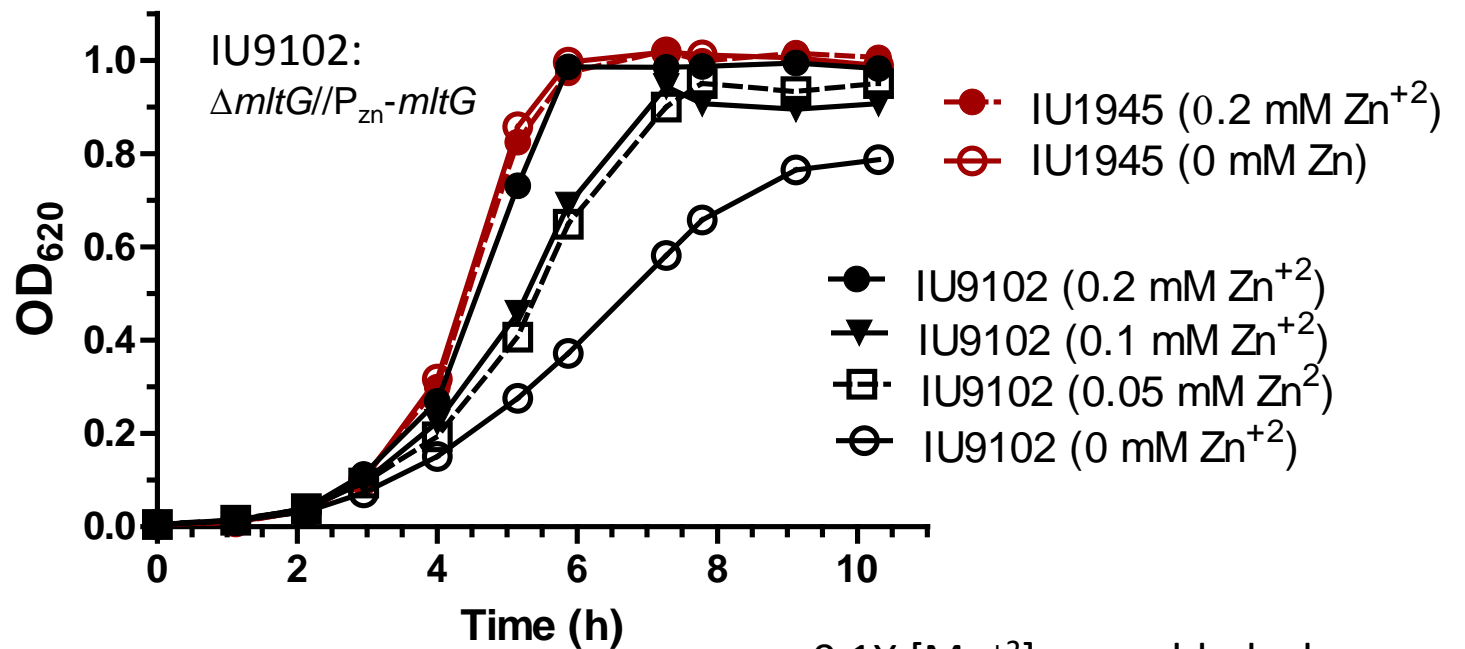


Fig. S9



0.1X [Mn²⁺] was added whenever Zn²⁺ was added.

Fig. S10

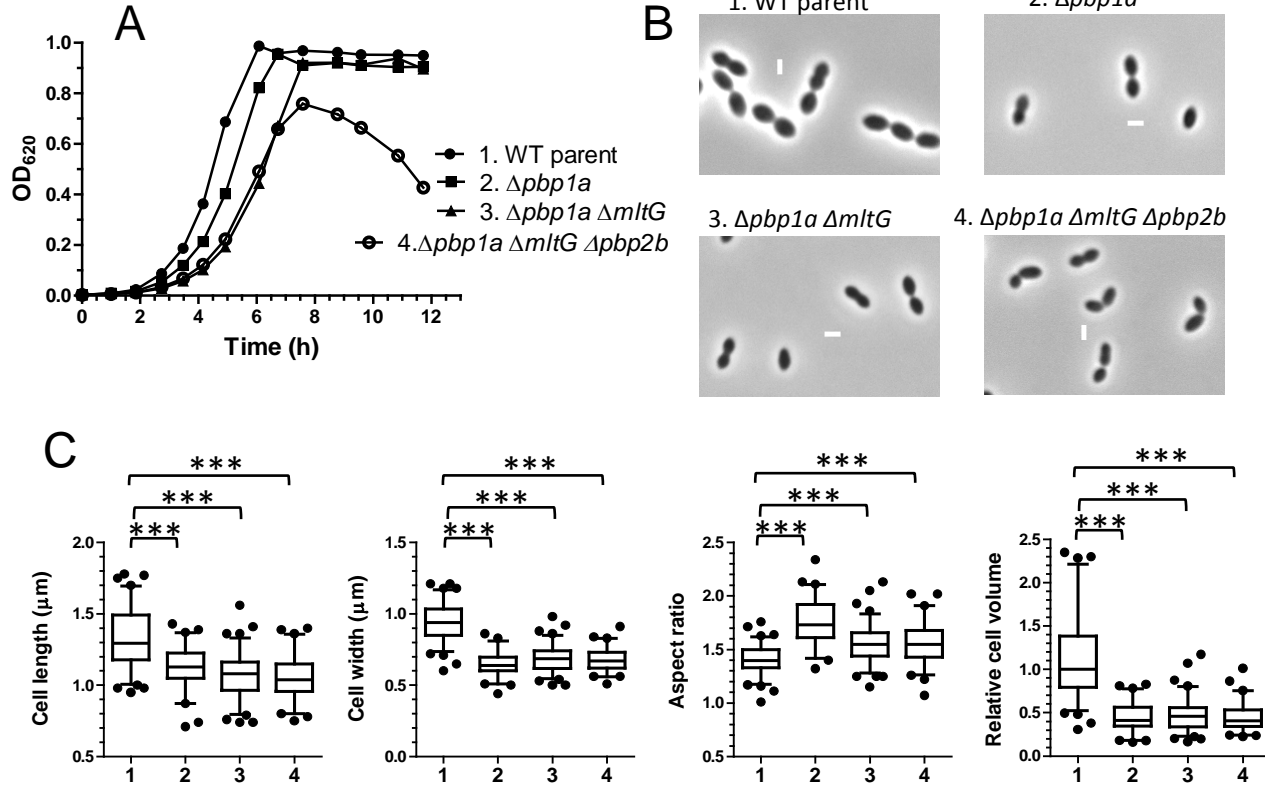


Fig. S11

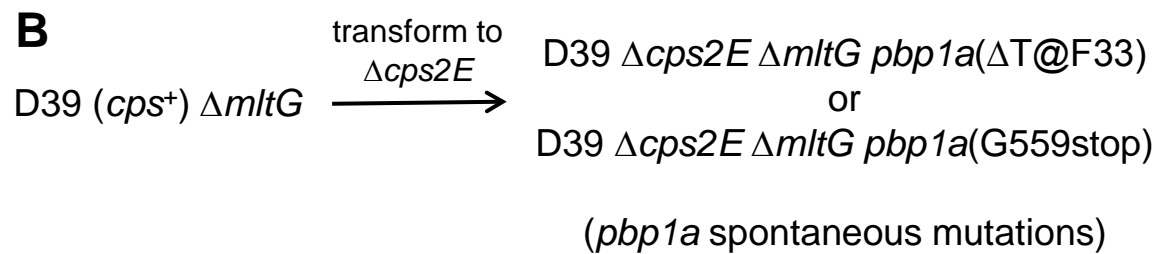
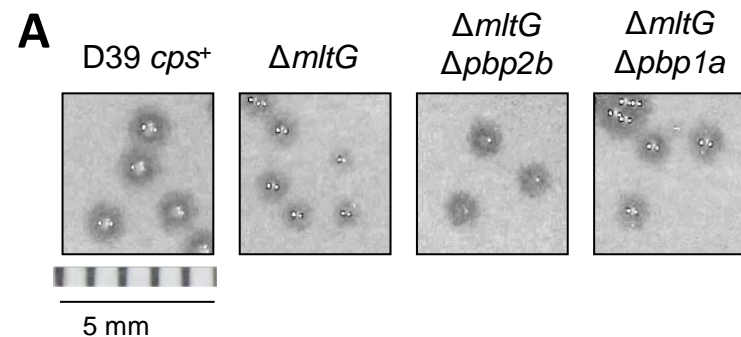


Fig. S12

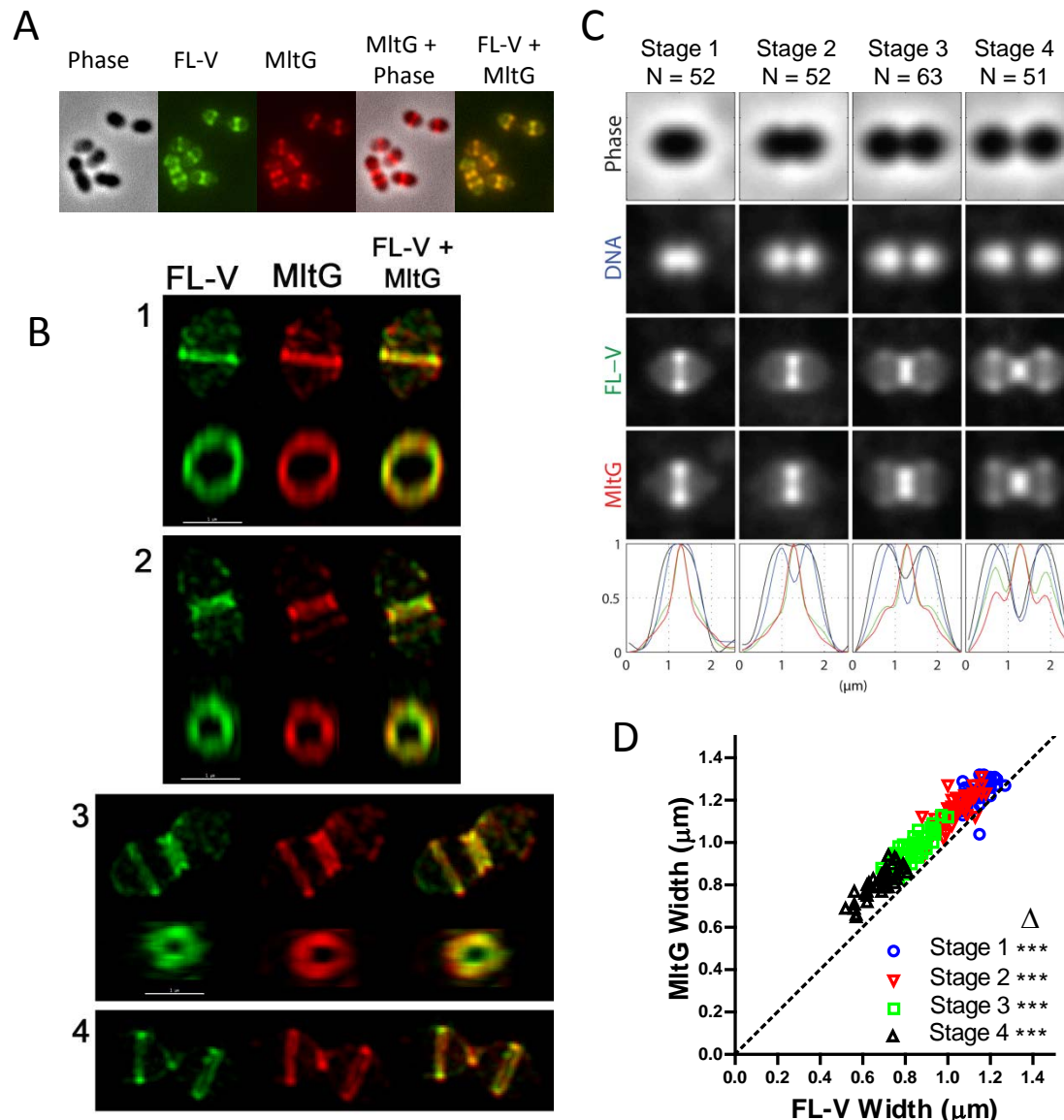


Fig. S13

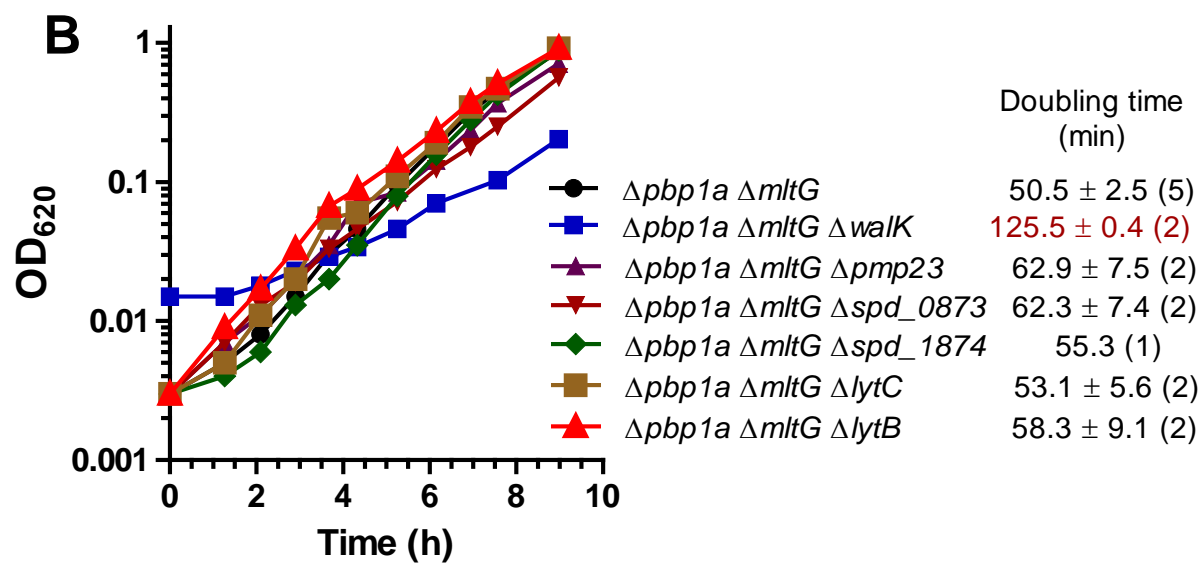
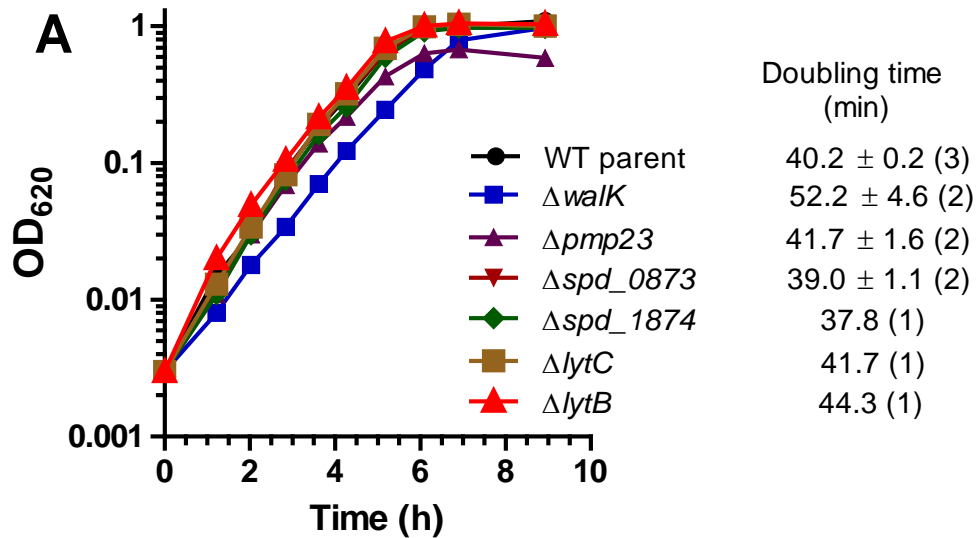


Fig. S14

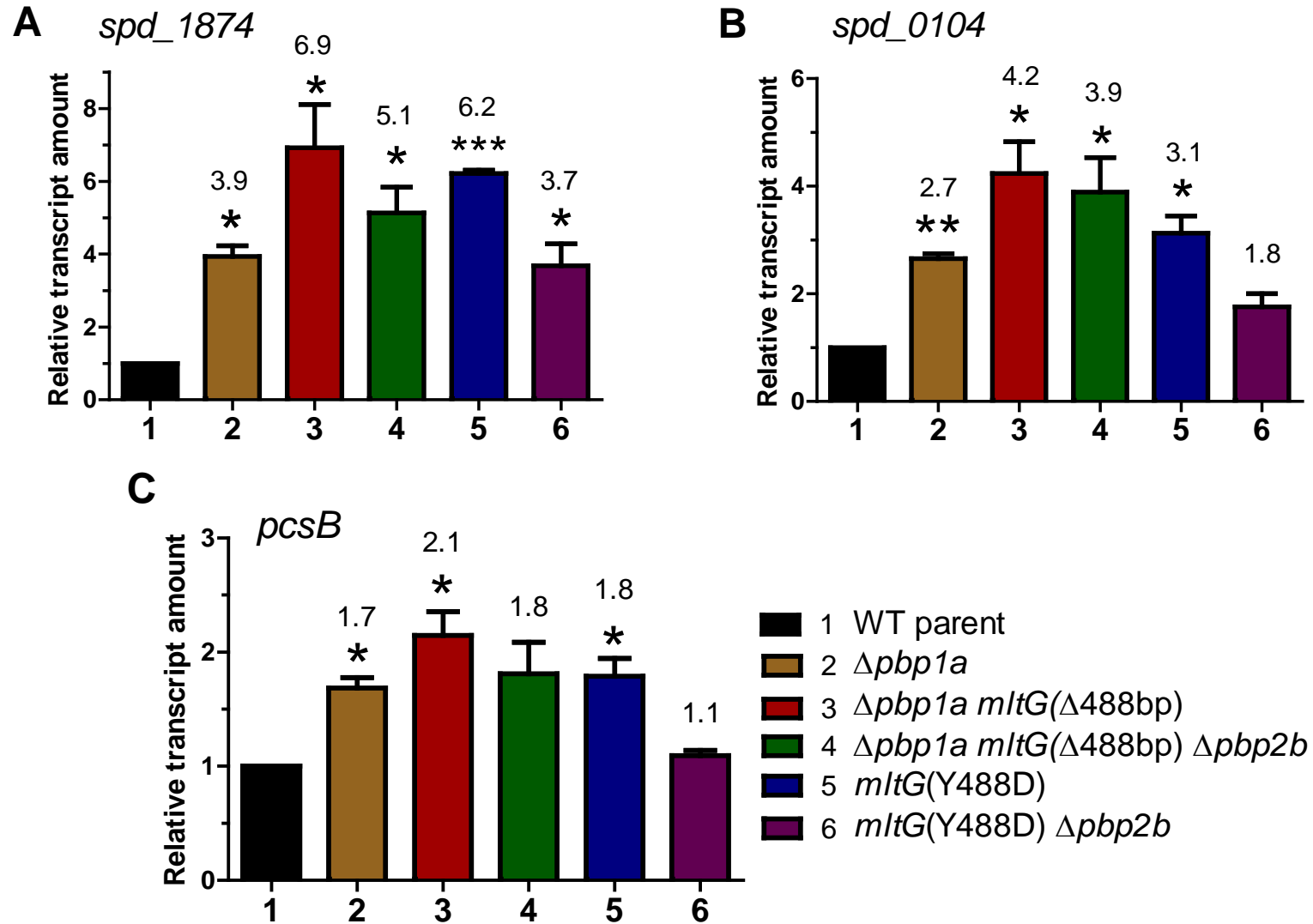


Fig. S15